Spatial Statistical Estimation and Classification — Theory and Applications from Centimeter to Continental Scale

Ute C. Herzfeld

Cooperative Institute for Research in Environmental Sciences
and
Department of Applied Mathematics
University of Colorado at Boulder
herzfeld@tryfan.colorado.edu

Spatial Statistical Methods for

(1) Estimation

(2) Classification

(3) Simulation

...with Applications in

Remote Sensing of Remote Locations —

Ice and Oceans

Examples from Centimeter to Continental Scale

→ scaling problems

→ surface roughness

Thanks to my collaborators and students ...

Koni Steffen, Roger Barry (CIRES), Jay Zwally, John DiMarzio (both NASA Goddard Space Flight Center), James Maslanik (CCAR, CU Boulder), Al Gasiewski (ETL, ECE, CU Boulder), Ron Kwok (JPL), John Heinrichs (Ft. Hays State Univ, KS), Robert Thomas (EG&G NASA GSFC Wallops), Robert Schutz (Univ Texas Austin), Don Cavalieri (NASA GSFC), Matthew Sturm (CRREL Ft. Wainworth), David Korn (NSIDC), Bruce Wallin, Steve Sucht, Danielle Lirette, Patrick McBride, Scott Williams, Chris Higginson, Michael Matassa (all CU Boulder and CIRES), Oliver Zahner, Matthias Mimler, Tim Erbrecht, Christoph Overbeck, Helmut Mayer, Sandra Boehm, Benno Rothstein, Ralf Stosius (all Geomathematik, Univ Trier), Wolfgang Feller (Techn Abt, Univ Trier), Nel Caine (Geography, CU Boulder), Michael Kuhn (Inst f Meteorologie und Geophysik, Univ Innsbruck), John Orcutt, Isaac Kim (IGPP, Scripps Inst of Oceanography), Jason Box (Byrd Polar Research Center, OSU)

... and for support through

- NASA Cryospheric Sciences (IPY Project)
- NSF Hydrological Sciences
- NSF Arctic Sciences
- ONR Acoustic Reverberation Special Research Project
- Deutsche Forschungsgemeinschaft (DFG), Antarctic and Arctic Research Program
- DFG, Heisenberg Fellowship
- Alexander von Humboldt Foundation, Feodor Lynen Fellowship
- CIRES, Visiting Fellows Program
- University of Colorado UROP Program

Geostatistical Estimation

Measurements $z_i(x)$, where $i = 1, \ldots, n$, on $z(x)$ are considered as a realization of a spatial random function $Z(x)$ for $x \epsilon D$ with the property that

$$(Z(x) - Z(x+h)) \quad \text{2nd-order stationary random function} \quad (1)$$

for fixed $h \epsilon \mathcal{R}^2$ such that $x, x+h \epsilon D$ (intrinsic hypothesis).

Hence the (semi-)variogram

$$\gamma(h) = \frac{1}{2} E[Z(x) - Z(x+h)]^2 \quad (2)$$

exists and is finite, γ measures the spatial continuity.

Variograms

In practice, an experimental variogram is calculated from a data set:

$$\gamma(h) = \frac{1}{2n} \sum_{i=1}^{n} [z(x_i) - z(x_i + h)]^2 \qquad (3),$$

where $z(x_i), z(x_i + h)$ are samples taken at locations x_i, $x_i + h \, \epsilon D$ respectively, where n is the number of pairs separated by $h \epsilon \mathcal{R}^2$.

To detect a drift component, m, calculate

$$m(h) = \frac{1}{n} \sum_{i=1}^{n} [z(x_i) - z(x_i + h)] \qquad (4)$$

and the "residual" variogram

$$res(h) = \gamma(h) - \frac{1}{2} m(h)^2 \qquad (5).$$

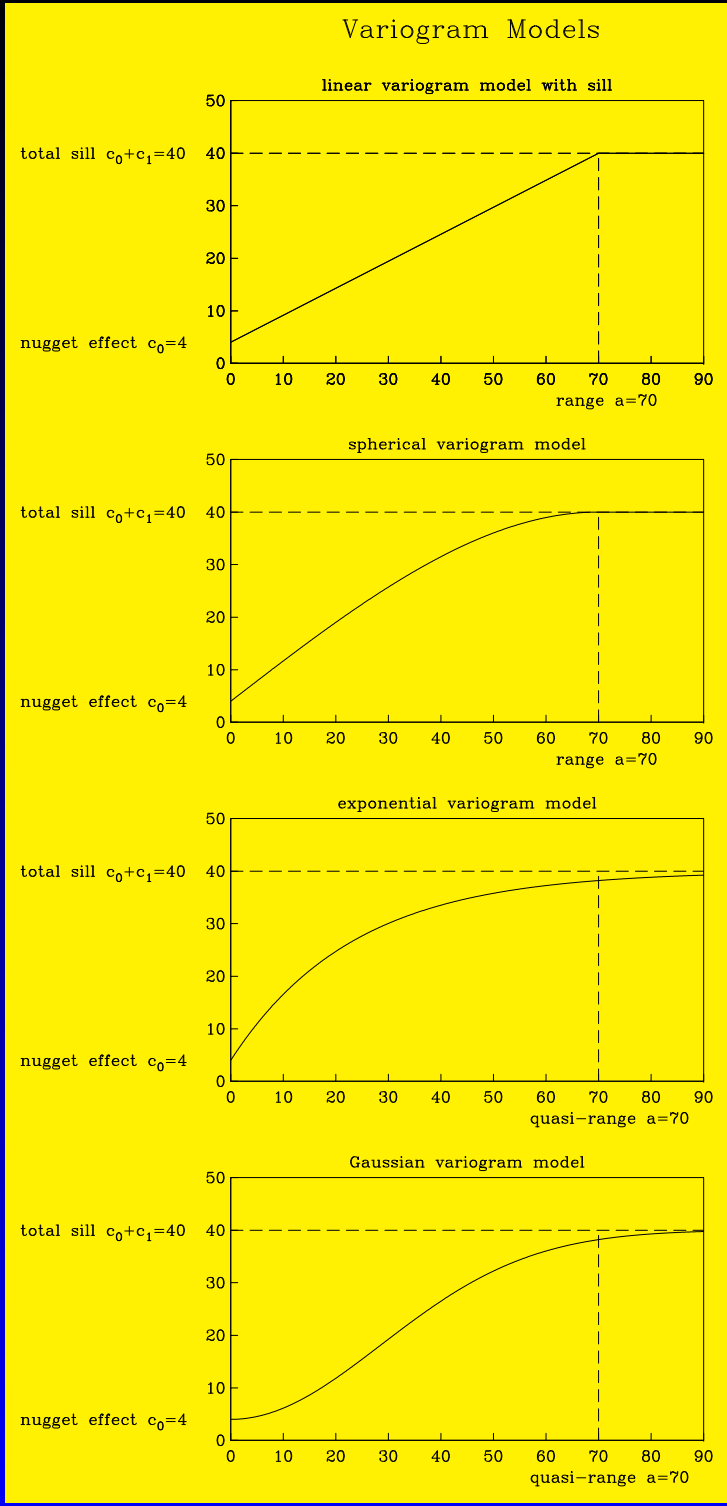
Variogram Models
linear variogram model with sill
total sill $c_0+c_1=40$
nugget effect $c_0=4$
range a=70
spherical variogram model
total sill $c_0+c_1=40$
nugget effect $c_0=4$
range a=70
exponential variogram model
total sill $c_0+c_1=40$
nugget effect $c_0=4$
quasi−range a=70
Gaussian variogram model
total sill $c_0+c_1=40$
nugget effect $c_0=4$
quasi−range a=70
0 10 20 30 40 50 60 70 80 90
0 10 20 30 40 50

Estimation: Kriging

Kriging is a family name for least-squares-based estimators.

$$Z_0^* = \alpha_0 + \sum_{i=1}^{n} \alpha_i \, Z(x_i) \quad \text{with} \quad \alpha_i \epsilon \mathcal{R} \qquad (6),$$

where weights are determined by a minimum variance criterion

$$E[Z_0^* - Z_0]^2 \quad \text{minimal !} \qquad (7)$$

and with respect to unbiasedness conditions $E[Z_0^* - Z_0] = 0$.

The estimation variance is (with $\varepsilon_0 = Z_0 - Z_0^*$)

$$\text{var}[\varepsilon_0] = \text{var}[Z_0] - 2 \sum_{i=1}^{n} \alpha_i \, \text{cov}[Z_0, Z_i] + \sum_{i,j=1}^{n} \alpha_i \, \alpha_j \, \text{cov}[Z_i, Z_j] \qquad (8)$$

IDEA:
Points closer by are better than points farther away

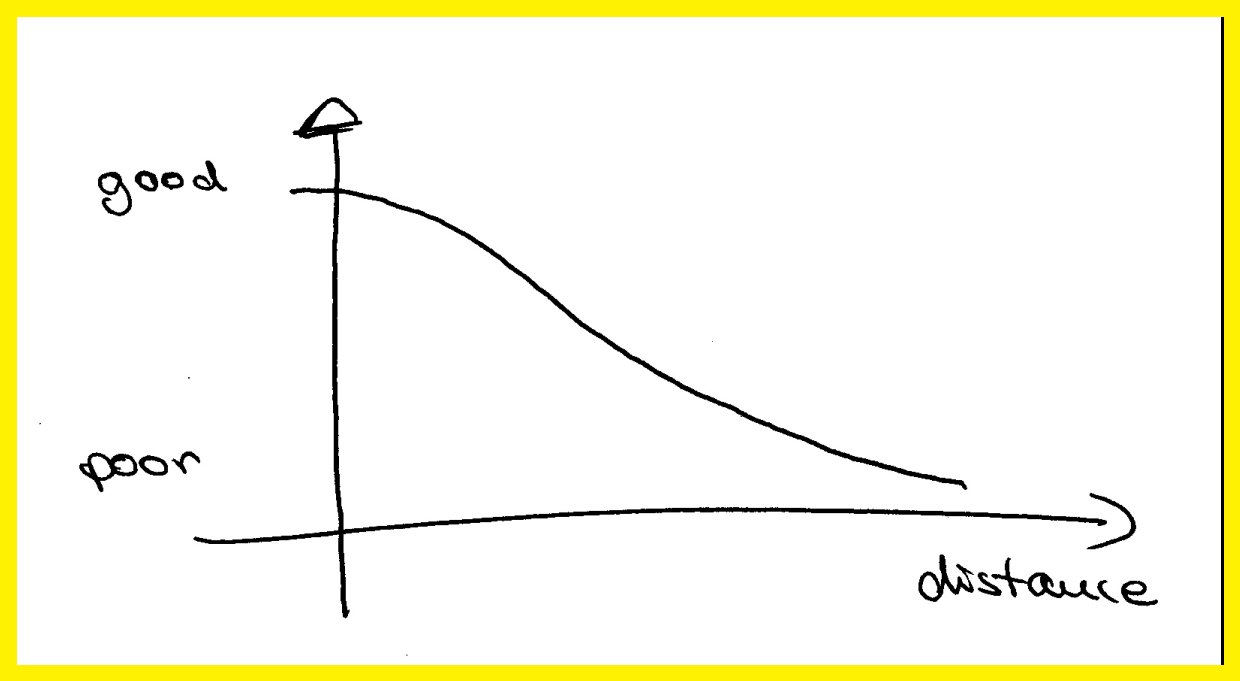

Variogram models are key to finding a solution of the inverse problem that

- is mathematically unique !!
- makes sense geologically !!

Solution

Using the notation

$$\gamma_{0i} = \gamma(x_0 - x_i)$$

$$\gamma_{ij} = \gamma(x_i - x_j)$$

for $i, j = 1, \ldots, n$ (9), minimization of the estimation variance yields a matrix equation (or n conditions). The unbiasedness conditions depend on the information available on the expectation of $Z(x)$.

(a) SIMPLE KRIGING: In case the expectations $E[Z(x_i)]$ are known for all $i = 1, \ldots, n$, the minimization is constrained by

$$\alpha_0 = E[Z(x_0)] - \sum_{i=1}^{n} \alpha_i \, E[Z(x_i)] \qquad (10).$$

This - practically rare - case is called *simple kriging*

Ordinary Kriging

Unknown but constant expectation $0 \neq E = E[Z(x)]$ for all $x \epsilon D$ leads to the unbiasedness condition

$$\sum_{i=1}^{n} \alpha_i = 1, \quad \alpha_0 = 0 \qquad (11).$$

OK Sytem

$$\begin{pmatrix} \gamma_{11} & \cdots & \gamma_{1n} & 1 \\ \vdots & \ddots & \vdots & \vdots \\ \gamma_{n1} & \cdots & \gamma_{nn} & 1 \\ 1 & \ldots & 1 & 0 \end{pmatrix} \begin{pmatrix} \alpha_1 \\ \vdots \\ \alpha_n \\ \lambda \end{pmatrix} = \begin{pmatrix} \gamma_{01} \\ \vdots \\ \gamma_{0n} \\ 1 \end{pmatrix} \qquad (12).$$

with λ a Lagrange parameter.

Universal Kriging

In case of an underlying trend, the process is split:

$$Z(x) = m(x) + Y(x) \tag{13}$$

into a deterministic drift component $m(x)$ and a residual random function $Y(x)$ which is second order stationary and has zero expectation and variogram γ^*.
Drift:

$$m(x) = \sum_{l=1}^{k} a_l \, f_l(x) \quad \text{for} \;\; k \epsilon \mathcal{N} \quad \text{and} \; a_l \epsilon \mathcal{R} \quad \text{for} \;\; l = 1, \ldots, k \tag{14},$$

in practise, the functions f_l are low-degree polynomials. Get k unbiasedness conditions:

$$\sum_{i=1}^{n} \alpha_i \, f_l(x_i) = f_l(x_0) \quad \text{for} \;\; l = 1, \ldots, k \tag{15}.$$

Solution: UK System

For instance, for a linear drift

$$m(x) = a_1 x_x + a_2 x_y \tag{16}$$

the (universal) kriging system is

$$\begin{pmatrix} \gamma^*_{11} & \dots & \gamma^*_{1n} & 1 & x_{1x} & x_{1y} \\ \vdots & \ddots & \vdots & \vdots & \vdots & \vdots \\ \gamma^*_{n1} & \dots & \gamma^*_{nn} & 1 & x_{nx} & x_{ny} \\ 1 & \dots & 1 & 0 & 0 & 0 \\ x_{1x} & \dots & x_{nx} & 0 & 0 & 0 \\ x_{1y} & \dots & x_{ny} & 0 & 0 & 0 \end{pmatrix} \begin{pmatrix} \alpha_1 \\ \vdots \\ \alpha_n \\ \lambda \\ a_1 \\ a_2 \end{pmatrix} = \begin{pmatrix} \gamma^*_{01} \\ \vdots \\ \gamma^*_{0n} \\ 1 \\ x_{0x} \\ x_{0y} \end{pmatrix} \quad (17).$$

The estimation variance is ($\lambda_1 = \lambda$, $\lambda_2 = a_1$, and $\lambda_3 = a_2$)

$$s^2 = \sum_{i=1}^{n} \alpha_i \, \gamma^*(x_i, x_0) + \sum_{l=1}^{k} \lambda_l \, f_l(x_0) \quad (18).$$

Marine Geophysics: Spectral interpolation of marine magnetic anomalies

Let $T(x,h)$ denote the marine magnetic anomaly at location x, where $x\epsilon\mathcal{R}^2$ and at observation level h.
Use upward/downward continuation $T(x,h)$ of $T(x,0)$ to a level h, where $h\epsilon\mathcal{R}^+$.
Consider a stochastic process $T(x,h)$ with

- - $T(x,h)$ Gaussian
- $T(x,h)$ stationary
- $E[T(x,h)] = 0$
- $T(x,h)$ harmonic
- the power spectral density, $S_T(k)$, of $T(x,0)$ can be estimated, where $k\epsilon\mathcal{R}^2$ is the wavenumber.

Caress and Parker (1989)

Upward continuation

$$T(x,h) = \int_{x\epsilon\mathcal{R}^2} \hat{T}(k,0)\, e^{-2\pi|k|h-2\pi ikx} d^2x = T(x,0) * e_h(x) \quad (1)$$

where

$$e_h(x) = \int_{x\epsilon\mathcal{R}^2} e^{-2\pi|k|h-2\pi ikx} d^2x \quad (2)$$

is the earth filter and $\hat{T}(k,0)$ denotes the Fourier transform of $T(x,0)$, *i.e.* the magnetic anomaly at level h is the convolution of the magnetic anomaly at level 0 with the earth filter associated to h. (Parker 1973)

For observations of $T(x,h)$ in locations x_j with noise σ_j for $j = 1, \ldots, n$, let

$$f_j(k) = e^{-2\pi|k|h - 2\pi i k x_j} \quad \text{for } k \epsilon \mathcal{R}^2 \qquad (3).$$

Define a scalar product:

$$< f, g >= \int\limits_{k \epsilon \mathcal{R}^2} f(k)\, \overline{g(k)}\, S_T(k) d^2 k, \qquad f, g \epsilon S(\mathcal{R}^2) \qquad (4),$$

using the power spectral density $S_T(k)$ of $T(x,0)$ and a norm $\|f\|$ with $\|f\|^2 =< f, f >$.

($S(\mathcal{R}^2)$ Hilbert space of bounded and integrable fctns in $\mathcal{R}^2$).

Spectral Estimate

The spectral estimate of $T(x_0, 0)$ in a prediction point $(x_0, 0)$ is

$$T^*(x_0, 0) = \sum_{j=1}^{n} \alpha_j \, T(x_j, h) \quad \text{with } \alpha_j \epsilon \mathcal{R}, \quad \text{for } j = 1, \ldots, n \tag{5}.$$

The estimation error at x_0 is

$$\varepsilon(x_0) = T(x_0, 0) - T^*(x_0, 0) = T(x_0, 0) - \sum_{j=1}^{n} \alpha_j \, T(x_j, 0) * e_h(x_j) \tag{6}.$$

Determine the optimal weights α_j for $j = 1, \ldots, n$ by minimization of the error variance. The variance of a process being the integral of its power spectral density in the wave-number-domain (Parseval's Theorem), we get

$$\mathrm{var}(\varepsilon) = \int\limits_{k \epsilon \mathcal{R}^2} S_T(k) \, |1 - \sum_{j=1}^{n} \alpha_j \, e^{-2\pi|k|h - 2\pi i k x_j}| \, d^2k \qquad (7)$$

Get weights from:

$$V = \|1 - \sum_{j=1}^{n} \alpha_j \, f_j\|^2 + \sum_{j=1}^{n} \alpha_j \, \sigma_j^2 \qquad (8).$$

Solution

The PSD is positive and hence the mx positive definite, so the spectral estimation system has unique solution $(\alpha_1, \ldots, \alpha_n)$:

$$\begin{pmatrix} \|f_1\|^2 + \sigma_1^2 & \ldots & < f_1, f_n > \\ \vdots & \ddots & \vdots \\ < f_n, f_1 > & \ldots & \|f_n\|^2 + \sigma_n^2 \end{pmatrix} \begin{pmatrix} \alpha_1 \\ \vdots \\ \alpha_n \end{pmatrix} = \begin{pmatrix} < f_1, 1 > \\ \vdots \\ < f_n, 1 > \end{pmatrix} \quad (SES)(9).$$

The estimation variance

$$V = \|1\|^2 - \sum_{j=1}^{n} \alpha_j \ < f_j, 1 > \quad (10),$$

depends on the power spectral density only.

Inverse-Theoretical Formulation

Scalar products for a Hilbert space setting of estimation methods:
(1) Using the variogram

$$\langle Z(x_i), Z(x_j)\rangle = \gamma(x_i, x_j) \tag{48}$$

(2) Using PSD:

$$< f, g >= \int\limits_{k\epsilon\mathcal{R}^2} f(k)\,\overline{g(k)}\,S_T(k)d^2k, \qquad f, g\epsilon S(\mathcal{R}^2) \qquad (4),$$

To simplify the analogy, let

$$\langle T(x_a, 0), T(x_b, 0)\rangle = \mathrm{cov}(T(x_a, 0), T(x_b, 0)) \qquad (4),$$

so the distance becomes the variance of the difference of the processes (by use of the Wiener-Kinchin-theorem).

Estimates as Minimum-Distance Solutions

$$Z_0^* = \alpha_0 + \sum_{i=1}^{n} \alpha_i \, Z(x_i)$$

$$T^*(x_0, 0) = \sum_{j=1}^{n} \alpha_j \, T(x_j, h)$$

are minimum-distance solutions in the sense of the projection theorem: Z^* and T^* (respectively) are characterized by

$$(\alpha_{i_0})_{i=1,\ldots,n} \text{ soln of Kriging system } \iff \|Z_0 - Z_0^*\| \text{ min}$$

$$(\alpha_{j_0})_{j=1,\ldots,n} \text{ soln of SES system } \iff \|T(x,0) - T^*(x,0)\| \text{ min}$$

Note that for (UK) the solution is searched in a submanifold, not a subspace, because of the unbiasedness conditions.

Recent Rapid Changes of the Cryosphere

- Glaciers in most mountain ranges retreat
- Antarctic and Greenland Ice Sheets lose elevation
- Outlet glaciers of ice sheets accelerate and retreat
- Northern Antarctic ice shelves break up
- Arctic sea-ice cover reaches record lows in coverage

Approach

Understanding Environmental Change through Spatial Statistical Analysis of Remote-Sensing Data

Satellite Altimetry

- Geophysical measurement of surface elevation from satellite, using active microwave radar technology or laser technology
- Satellites with radar altimeters

(1) SEASAT (1978)
(2) GEOSAT (1985–1989)
(3) ERS-1 (1991-1996)
(4) ERS-2 (since 1995)
(5) TOPEX/POSEIDON
(6) JASON-1/2
(7) ENVISAT (since 2002)

- Satellite with laser altimeters

ICESat: GLAS (since 2003)

Processing of Altimeter Data

1. “Retracking", identification of ground position for returns
2. Transformation of waveform data record into ice data records
3. Correction for atmospheric effects
4. Correction for solid Earth tides
5. Slope correction of the ice surface
6. Correction for water vapor
7. Referencing to GEM-T2 satellite orbits
8. Resulting in elevations in meters above the WGS-84 ellipsoid

(Example: ERS-1 data processing by Ice Sheet Altimetry Group, NASA Goddard Space Flight Center, J. Zwally, J. DiMarzio and coworkers)

GEOSAT ERM Ground Tracks

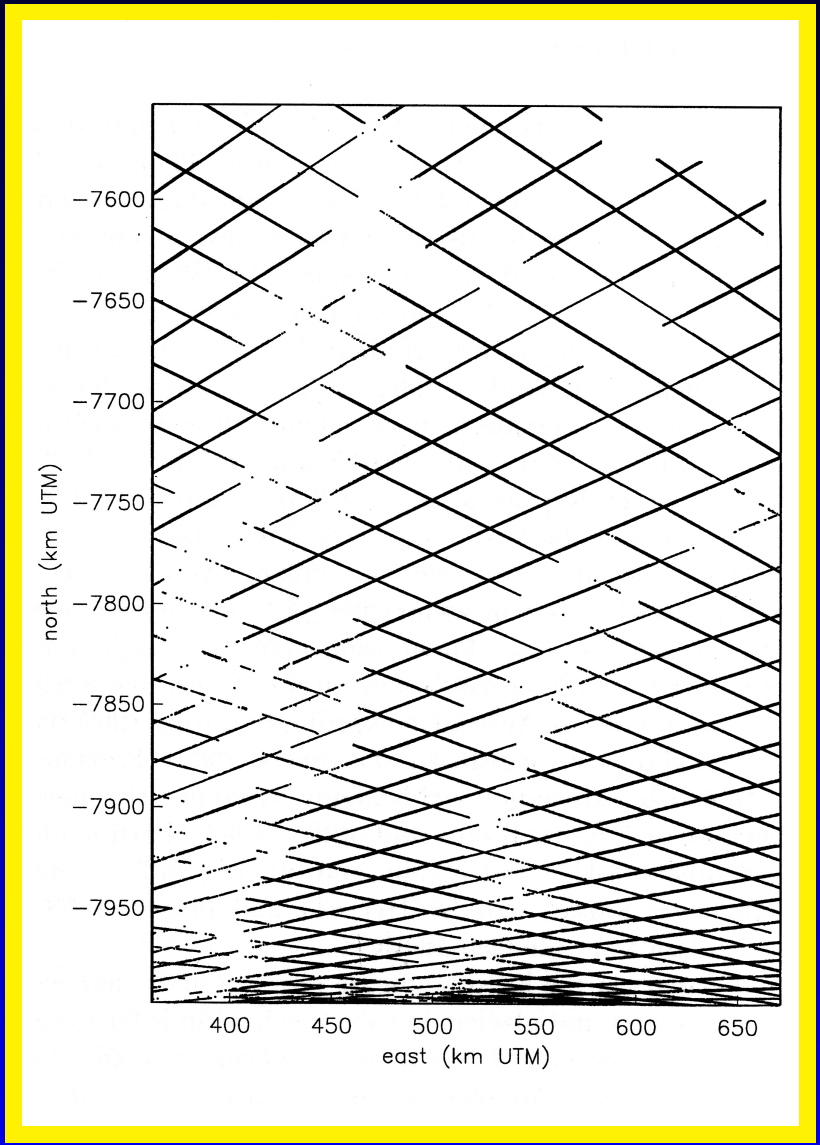

Surface Elevation of Lambert Glacier/Amery Ice Shelf System

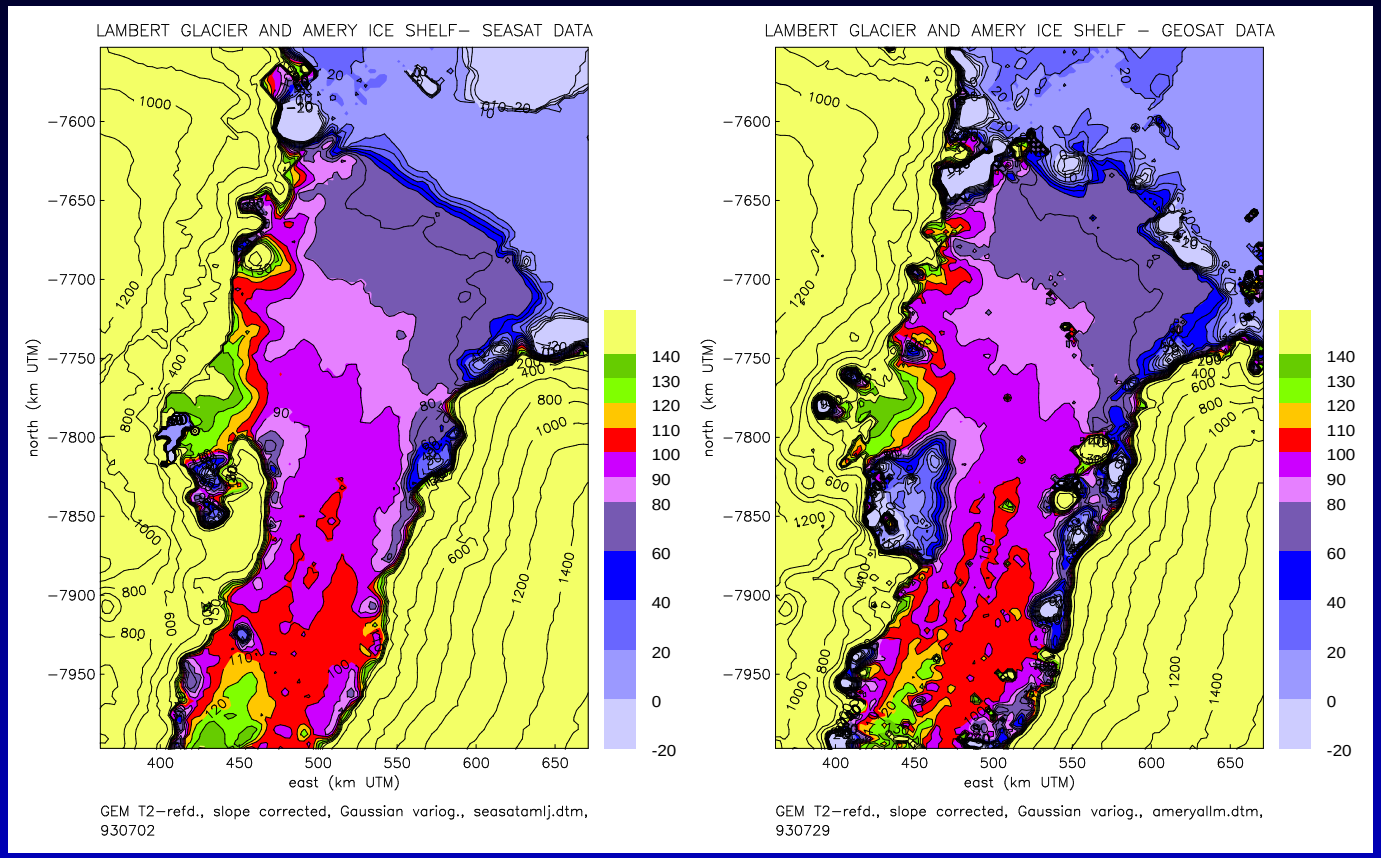

Comparison of SEASAT (1978) and Geosat (1987-1989) data using geostatistical evaluation indicates growth of ice stream:

- increase of surface elevation
- advance of grounding line by $\approx$ 400 m/yr

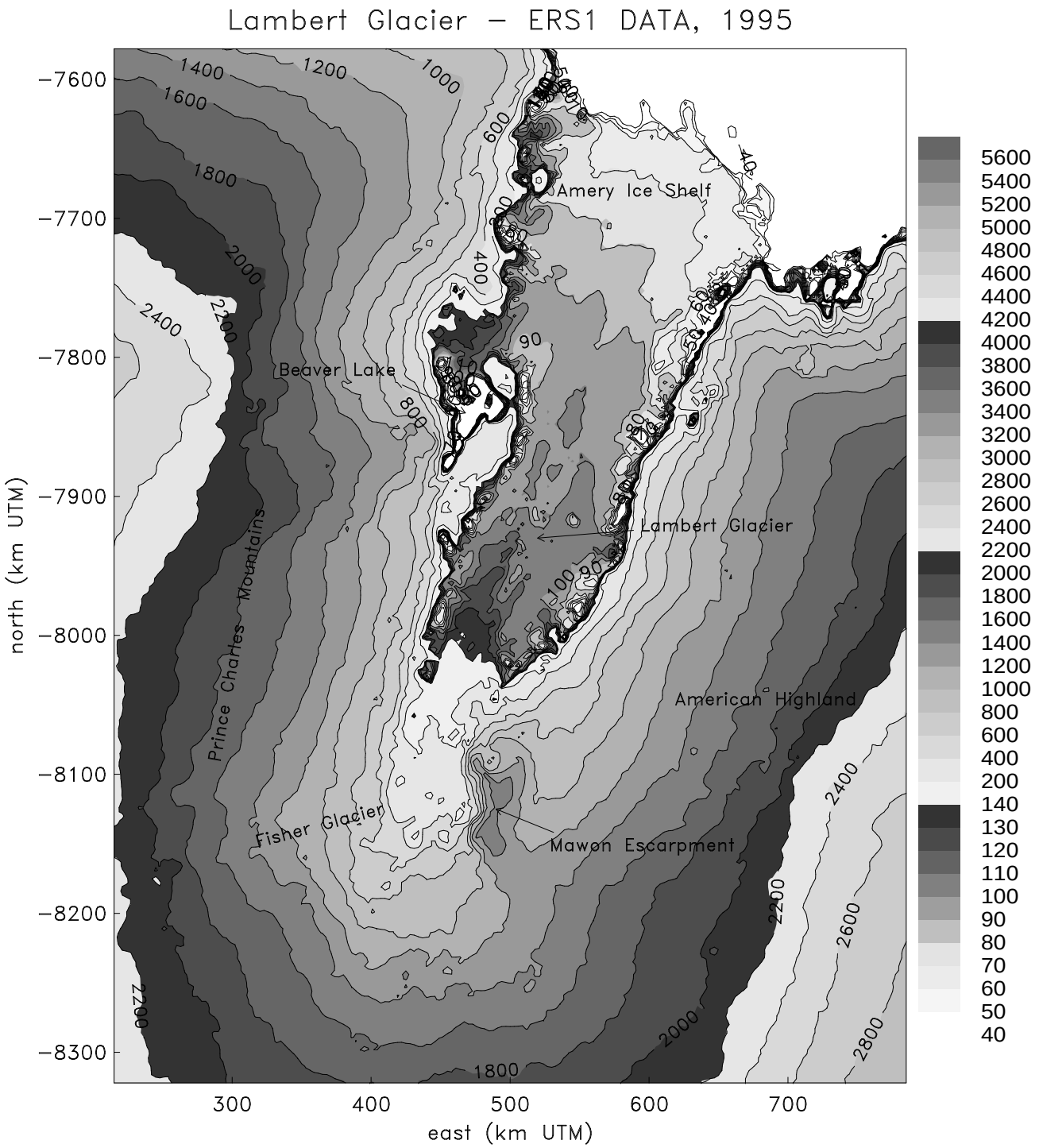

e59−79n68−75, WGS84, Gaussian variog., central mer. 69, slope

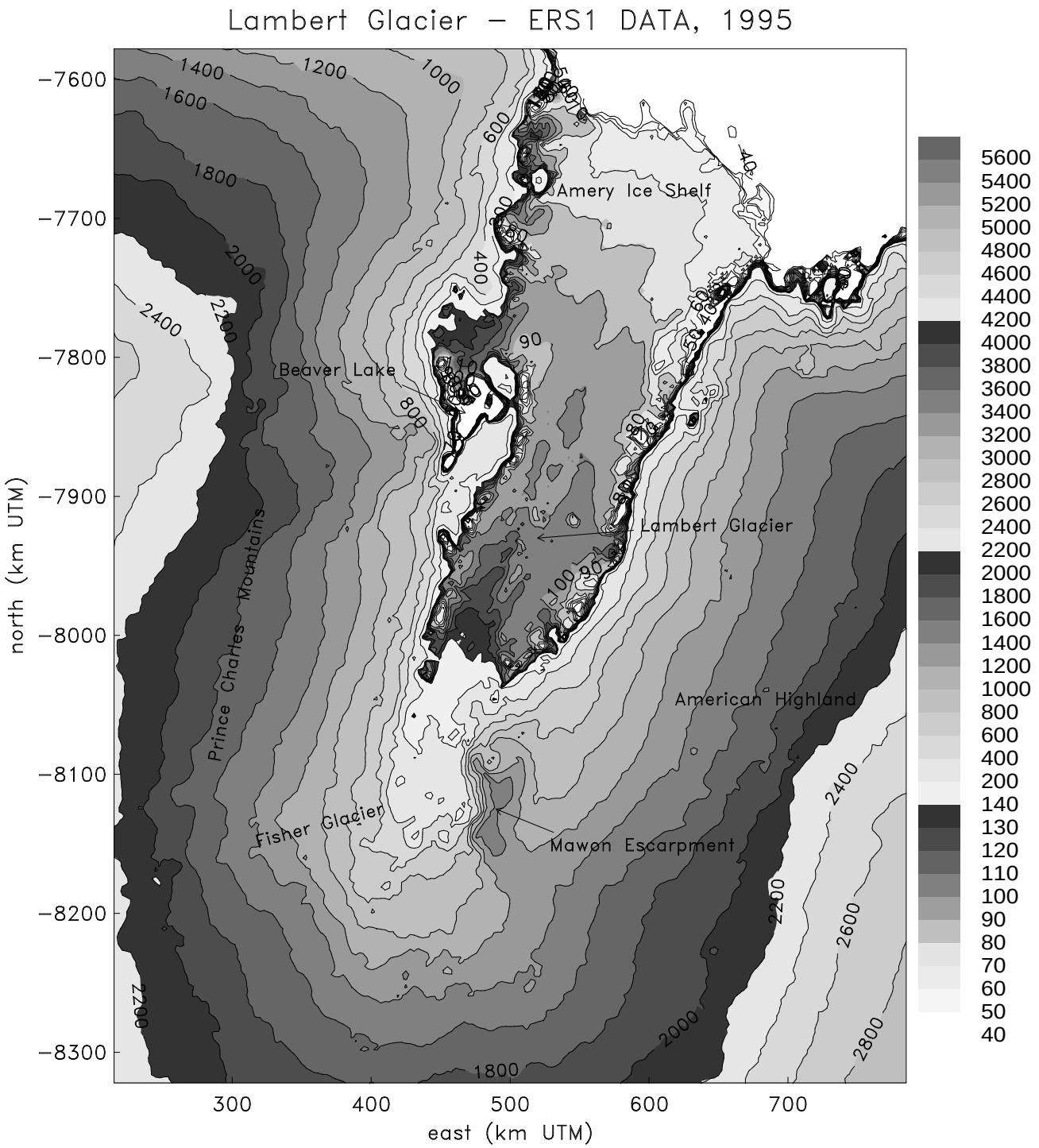

e59−79n68−75, WGS84, Gaussian variog., central mer. 69, slope

Topography and Flowlines of Lambert Glacier/Amery Ice Shelf System

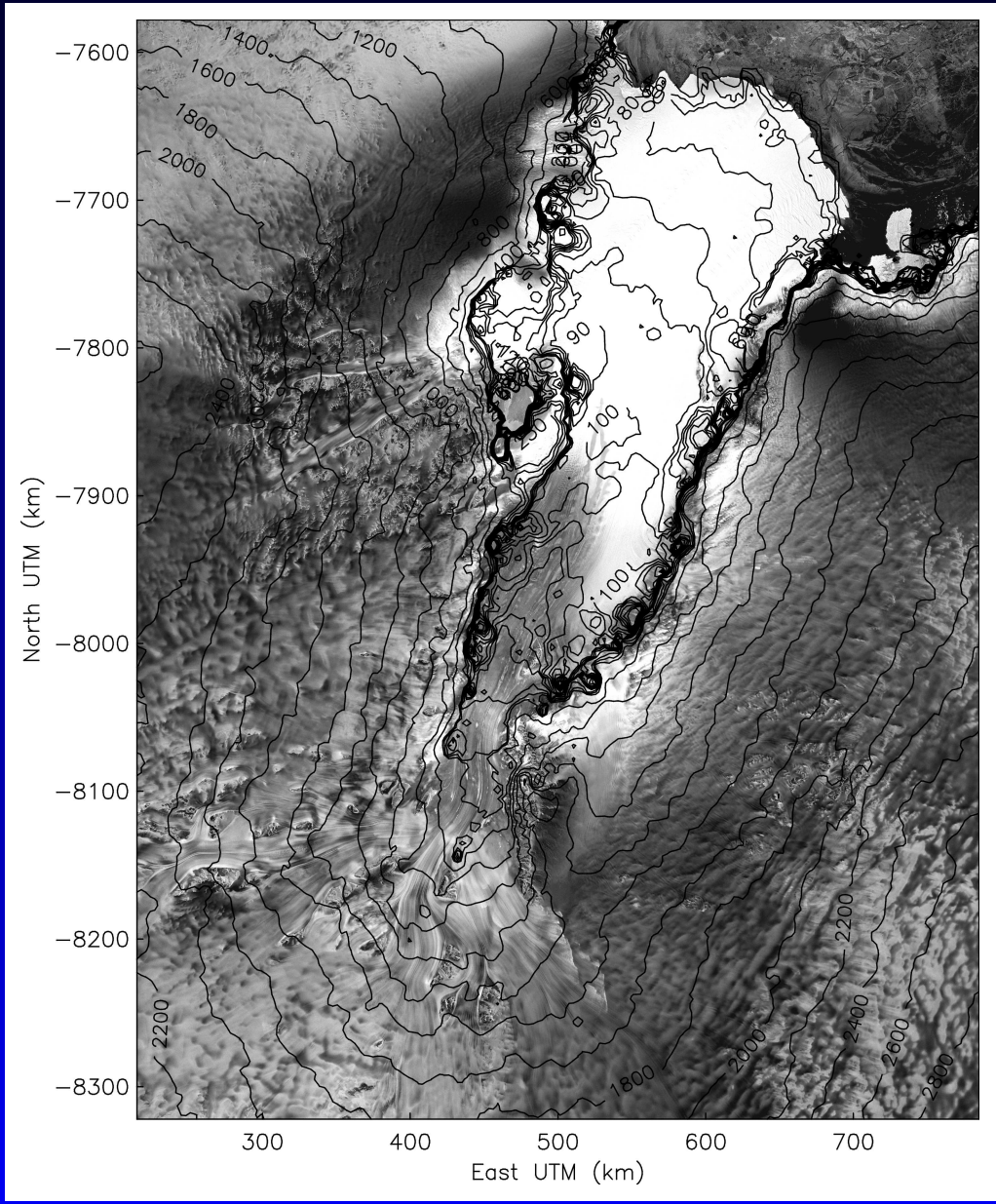

Elevation:

1997 ERS-2 data (1 Aug–31 Oct 1997), geostatistical analysis (Herzfeld et al.)

Surface Structure:

1997 RADARSAT data (RADARMAP 1st Antarctic mission, 2 Sept- 20 Oct 1997; Mosaic Jezek et al., 125m pixels)

Data integration and geo-referencing:

Stosius and Herzfeld

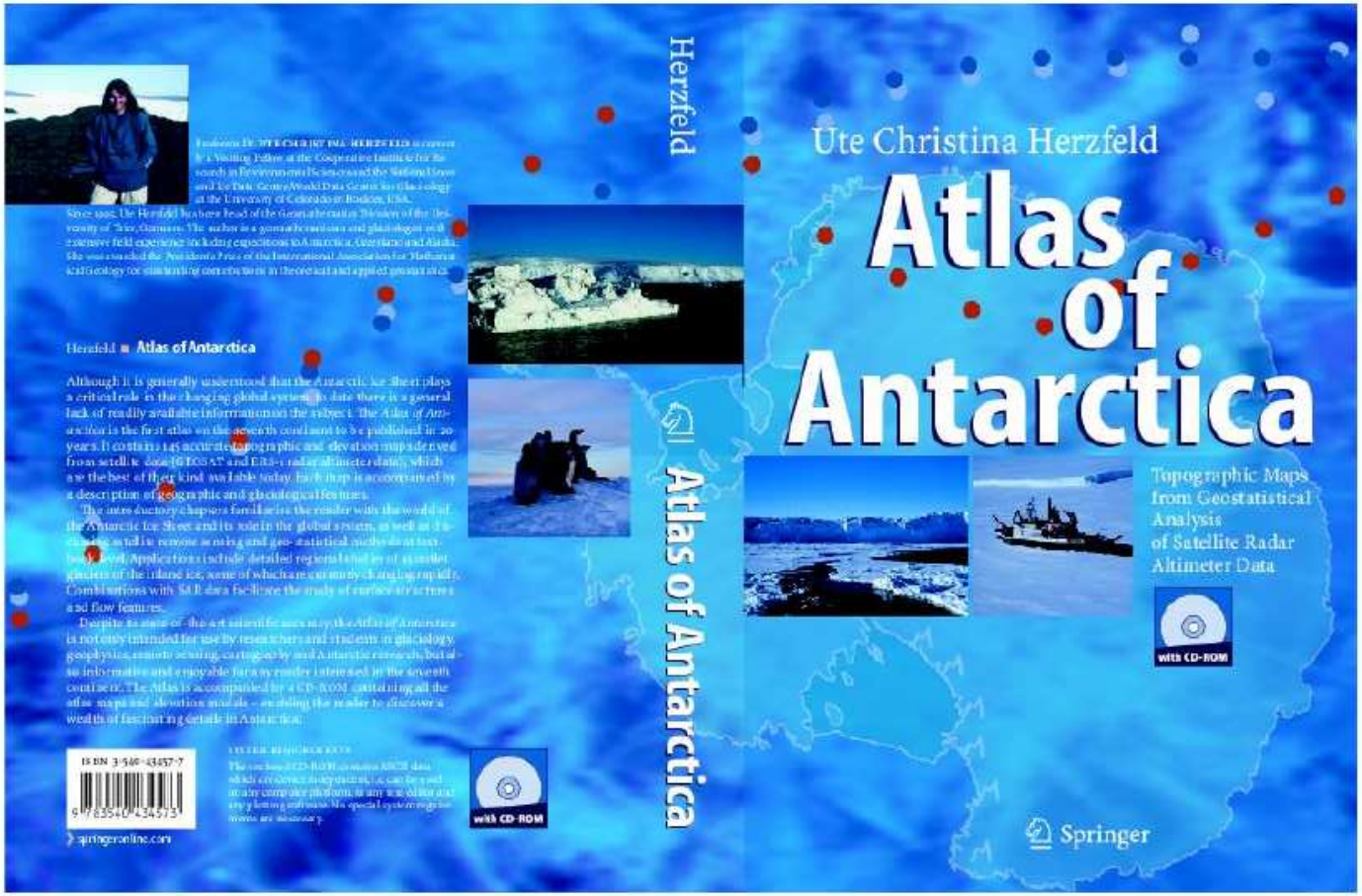
Herzfeld
Atlas of Antarctica
with CD-ROM
Herzfeld ■ Atlas of Antarctica
springeronline.com
Ute Christina Herzfeld
Atlas of Antarctica
Topographic Maps from Geostatistical Analysis of Satellite Radar Altimeter Data
with CD-ROM
Springer

Topics in Marine Research

- Marine Primary Production – Nutrient Cycles
- El Nino Southern Oscillation
- Discovery of the Antarctic Continental Margin
- Geologic History of the Seafloor
- Marine Geophysics
- Survey of the Gravity Field
- Seafloor Topography and Altimetry of the Sea Surface

Geologic Provinces on the Western Flank of the Mid-Atlantic Ridge at 26° North

HYDROSWEEP bathymetric data collected during cruise EW9208 with R/V Maurice Ewing, Lamont-Doherty Geological Observatory, 14 July-18 Aug 1992

Chief Scientists: B. Tucholke, M. Kleinrock, WHOI;

Funding: ONR Acoustic Reverberation Special Research Project, PI: J. Orcutt, SIO

Objectives

(1) Characterization of seafloor provinces: Establish a unique quantitative description of each surface type

(2) Classification: Assign a given object to a surface class, using the characterization

(3) Segmentation: Create a thematic map (a geologic map) by applying the classification operator in a moving window

Geostatistical Classification

Steps:

(1) Select a window in the study area

(2) Calculate vario function(s) for data in the window

(3) Filter the function in (2) [optional]

(4) Calculate vario parameters (geostatistical classification parameters) from (2) or (3)

(5) Compose a feature vector of parameters

(6) Associate the surface in the window (1) to a class by

  (a) deterministic algorithm

  (b) connectionist association (neural net)

Typical Experimental Variograms

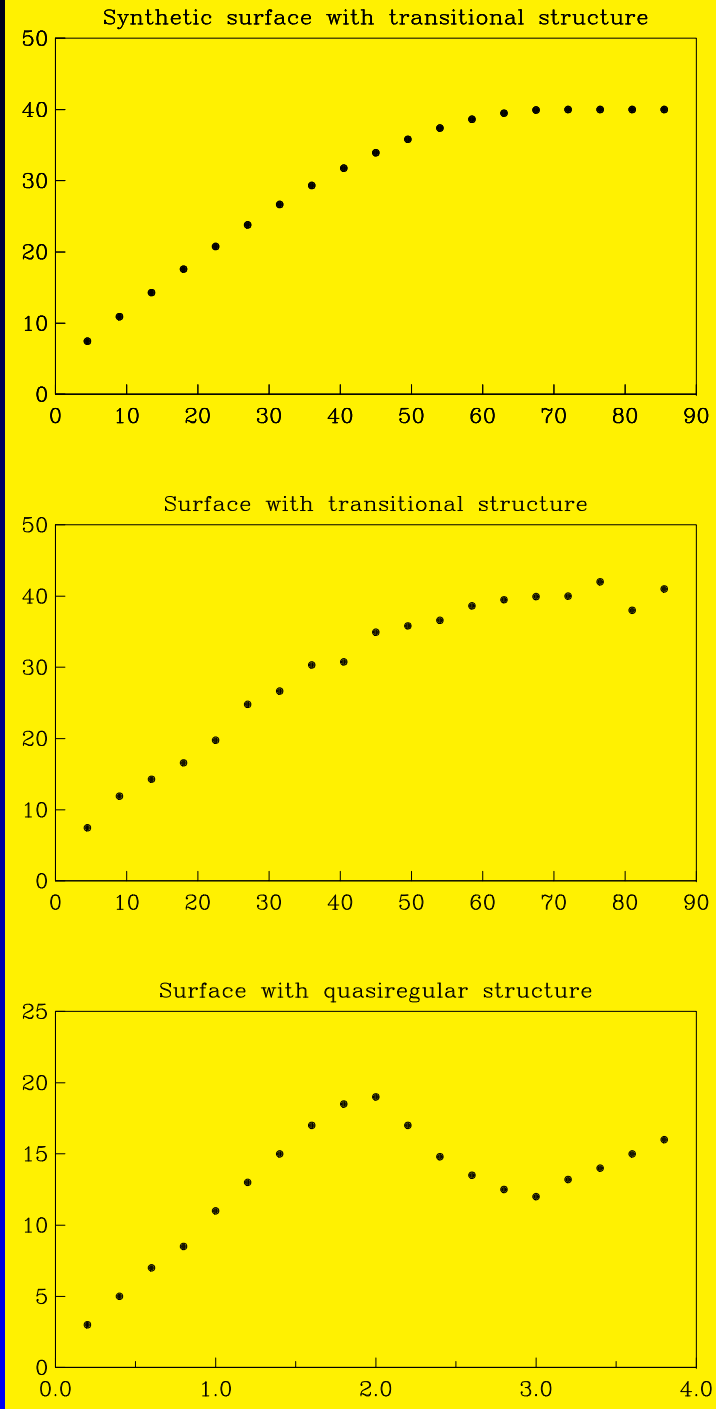

Geostatistical Classification Parameters

significance parameters:
slope parameter:

$$p1 = \frac{\gamma_{max_1} - \gamma_{min_1}}{h_{min_1} - h_{max_1}}$$

relative significance parameter:

$$p2 = \frac{\gamma_{max_1} - \gamma_{min_1}}{\gamma_{max_1}}$$

pond – maximum vario value
mindist – distance to first min after first max

$$avgspac = \frac{1}{n} \sum_{i=1}^{n} \frac{1}{i} h_{min_i}$$

Geostatistical Seafloor Classification

Parameter $mindist$

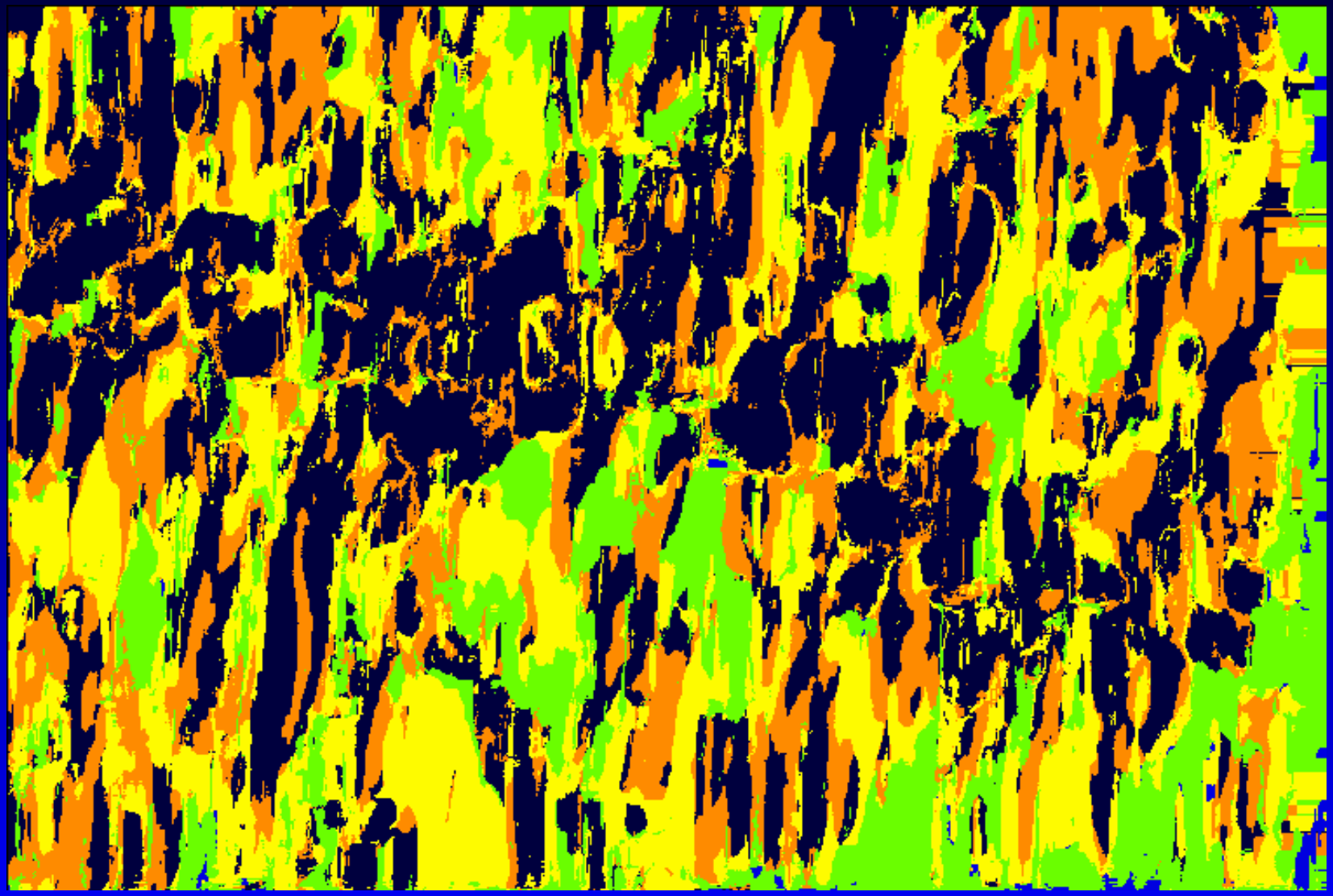

Geostatistical Seafloor Classification

Parameter $p1$:
significance of abyssal hill terrain (slope)

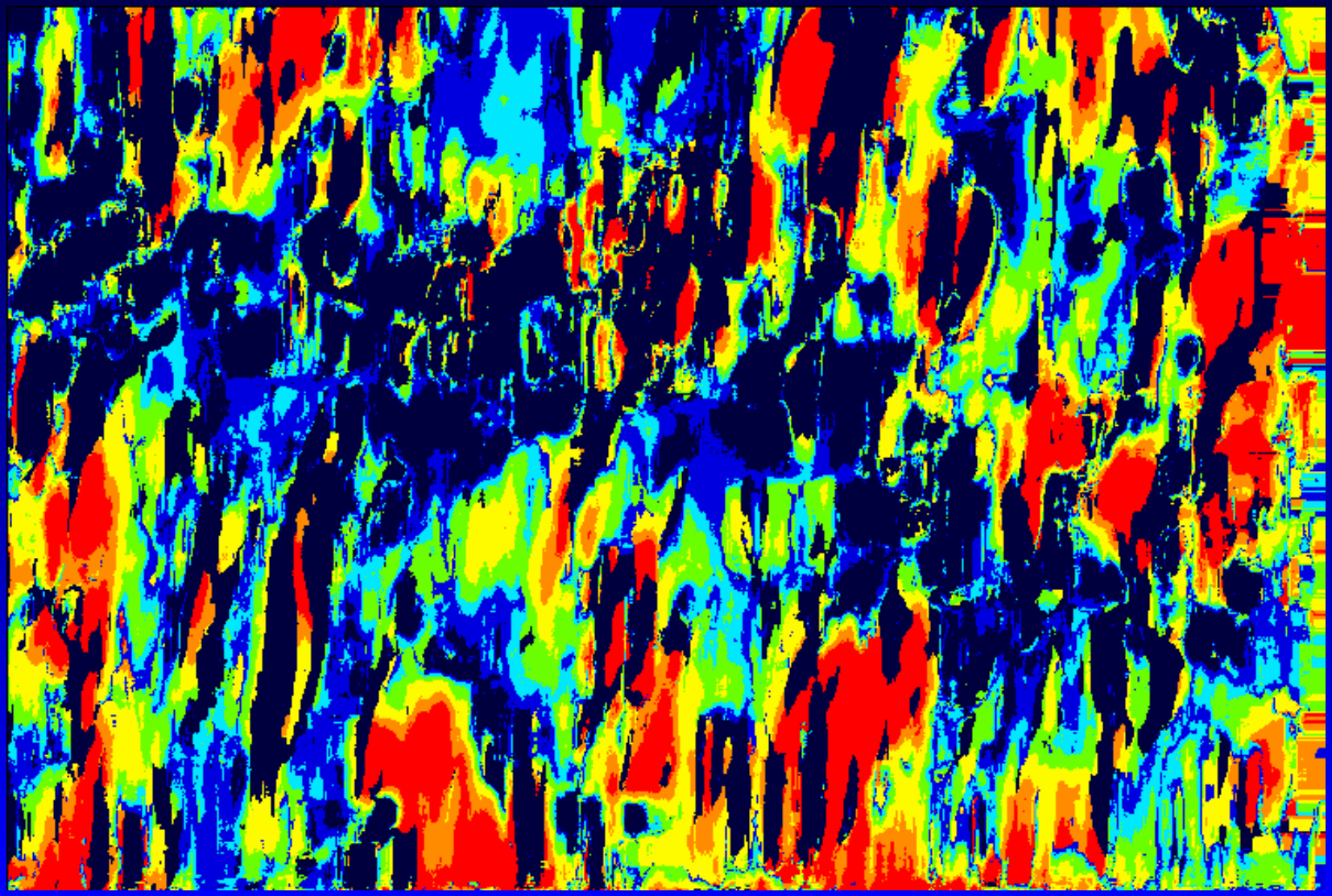

Geostatistical Seafloor Classification

Parameter $p2$:
significance of abyssal hill terrain (relative size)

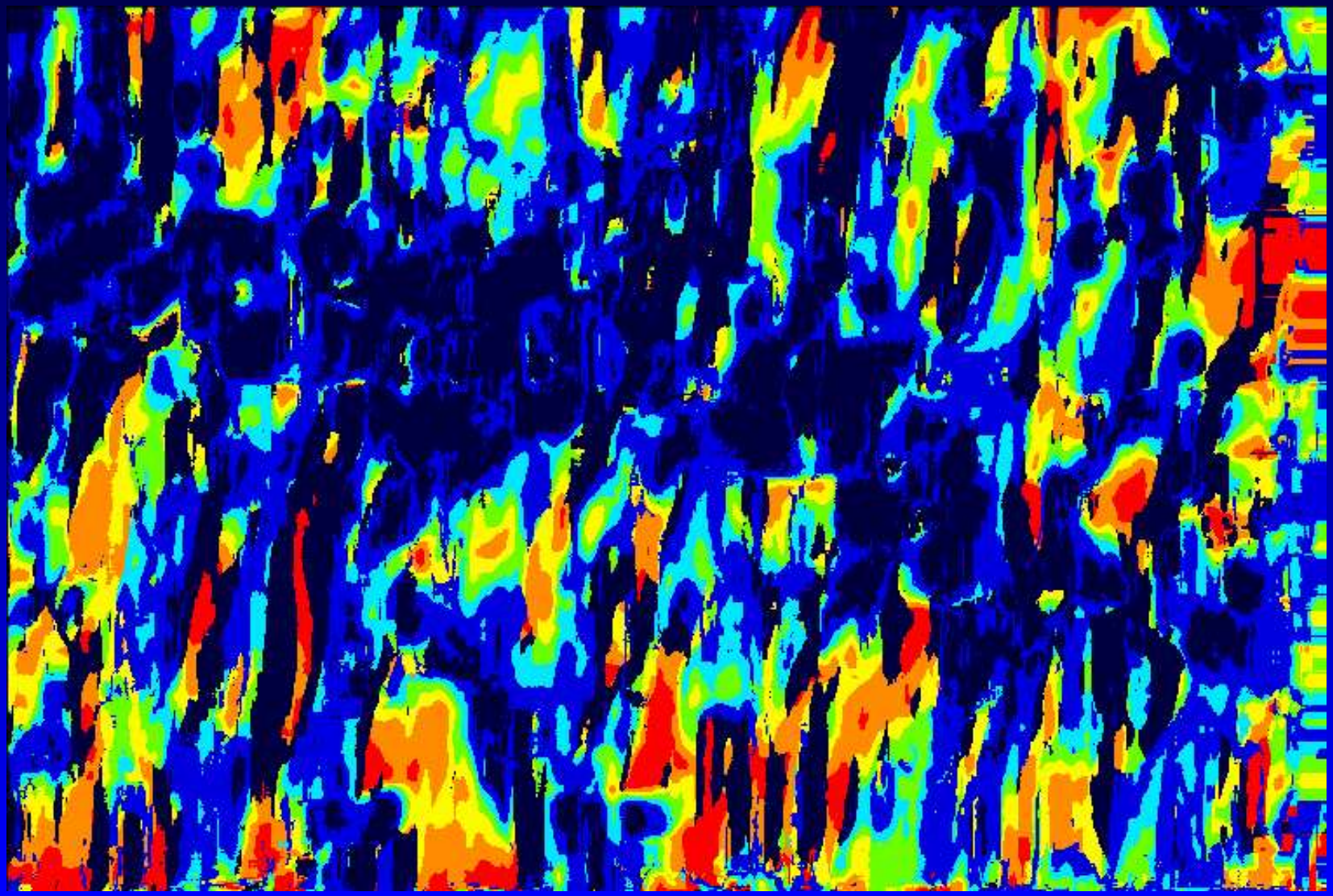

Geostatistical Seafloor Classification

Parameters $pond$ and $mindist$

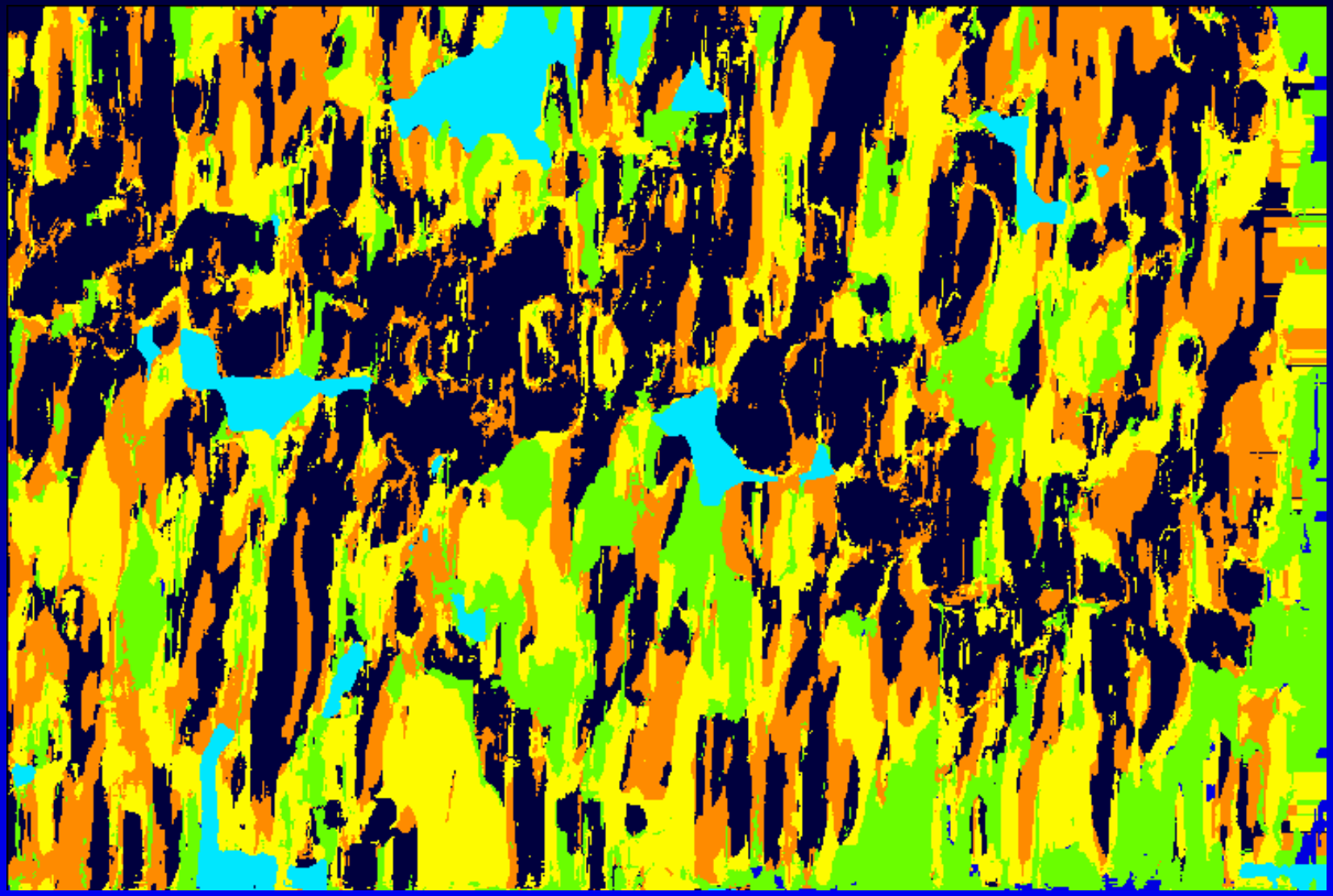

Concept and Analysis of Spatial Surface Roughness

Mathematical objective:

– Realize new methodological components for spatial structure analysis

– Identify, characterize and classify forms from hidden information in

(a) Undersampled situations

(b) Oversampled situations

Glaciologic objective:

Detect and quantify different forms of change in the cryosphere and attribute changes to glaciologic or sea-ice-morphogenetic processes

Remote-sensing objective:

Present and analyze observations from new instruments with a focus on the role of ICESat GLAS data

(1.) What is spatial surface roughness?

- a derivative of (micro)topography

$\longrightarrow$ characterization of spatial behavior

(2.) Why do we need surface roughness?

- morphologic characteristics are captured in surface roughness (*not* in absolute elevation)
- subscale information for satellite data

Niwot Ridge Snow Surface: Winter ——————— Summer

Bering Glacier, 1994, mature surge stage, Khittrov Hills in background

Jakobshavn Isbræ Drainage Basin – Spring Ice Surface

Jakobshavn Isbræ Drainage Basin – Summer Ice Surface

Jakobshavns Isbræ: August 1996

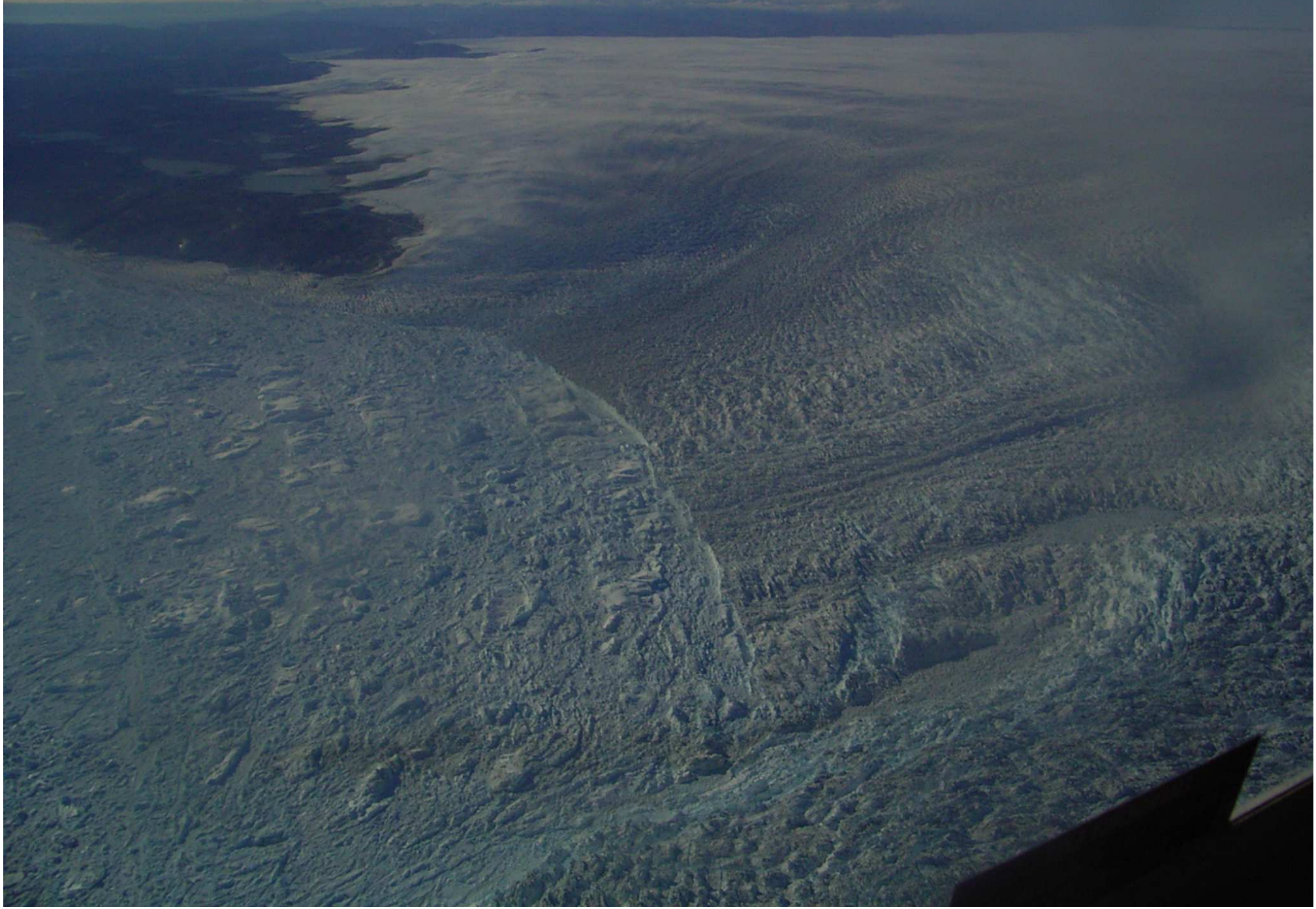

Calving Front of Jakobshavns Isbræ on 16 July 2005

(3.) How do we measure surface roughness? — The GRS !

A UAV with laser profilometer over Barrow

GRS Data – Greenland Ice Sheet

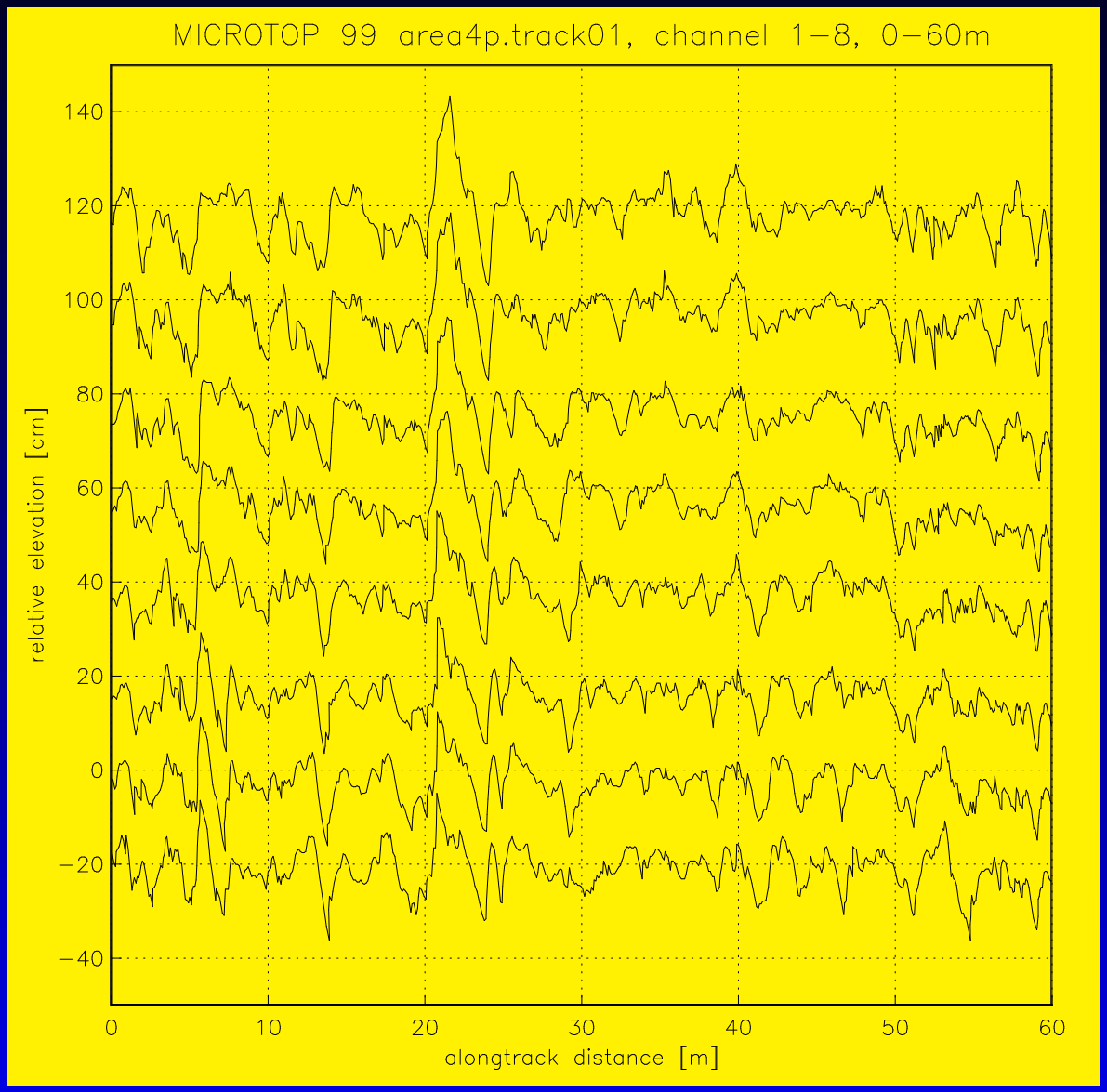

(4.) How do we analyze surface roughness?

The analytically defined spatial derivative needs to be calculated numerically from a data set.
One way to do this:

$$\lim_{x \to x_0} \frac{z(x_0) - z(x)}{x_0 - x}$$

surface slope in a given location x_0

To characterize morphology, better use averages...

Definition of Vario Functions

$V = \{(x, z)$ with $x = (x_1, x_2)\epsilon\mathcal{D}$ and $z = z(x)\} \subseteq \mathcal{R}^3$

discrete-surface case or

$$V = \{(x, z) \text{ with } x\epsilon\mathcal{D} \text{ and } z = z(x)\} \subseteq \mathcal{R}^2$$

discrete-profile case
Define the *first-order vario function* v_1

$$v_1(h) = \frac{1}{2n}\sum_{i=1}^{n}[z(x_i) - z(x_i + h)]^2$$

with $(x_i, z(x_i)), (x_i + h, z(x_i + h))\epsilon\mathcal{D}$ and n the number of pairs separated by h.

Higher-Order Vario Functions

The *first-order vario-function set* is

$$V_1 = \{(h, v_1(h))\} = \underline{v}(V_0)$$

Then: get V_2 from V_1 in the same way you get V_1 from V_0. The second-order vario function is also called *varvar function*.

Recursively, the *vario function set of order* $i+1$ is defined by

$$V_{i+1} = \underline{v}(V_i)$$

for $i \epsilon \mathcal{N}_0$.

GRS Data – Variogram

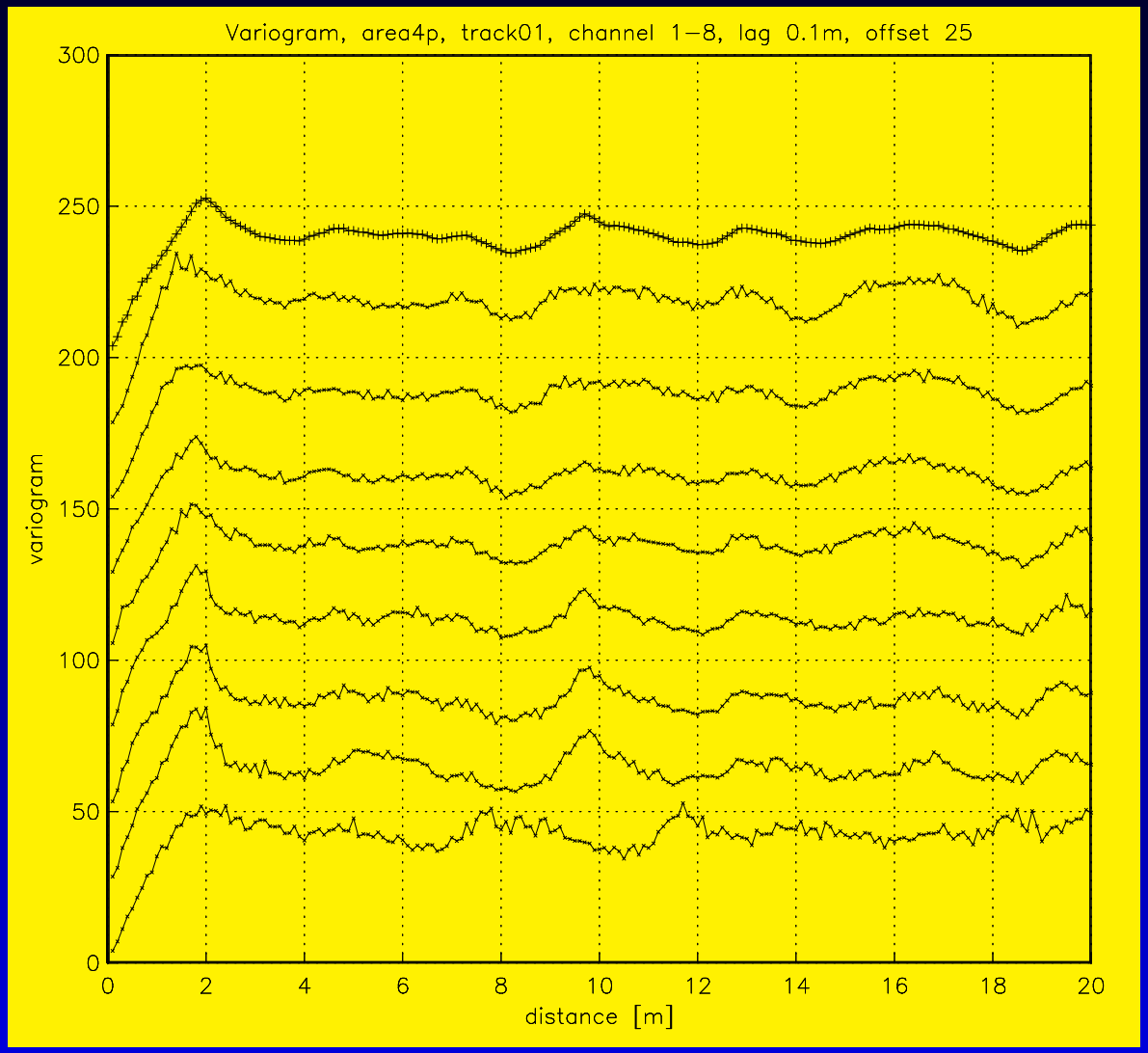

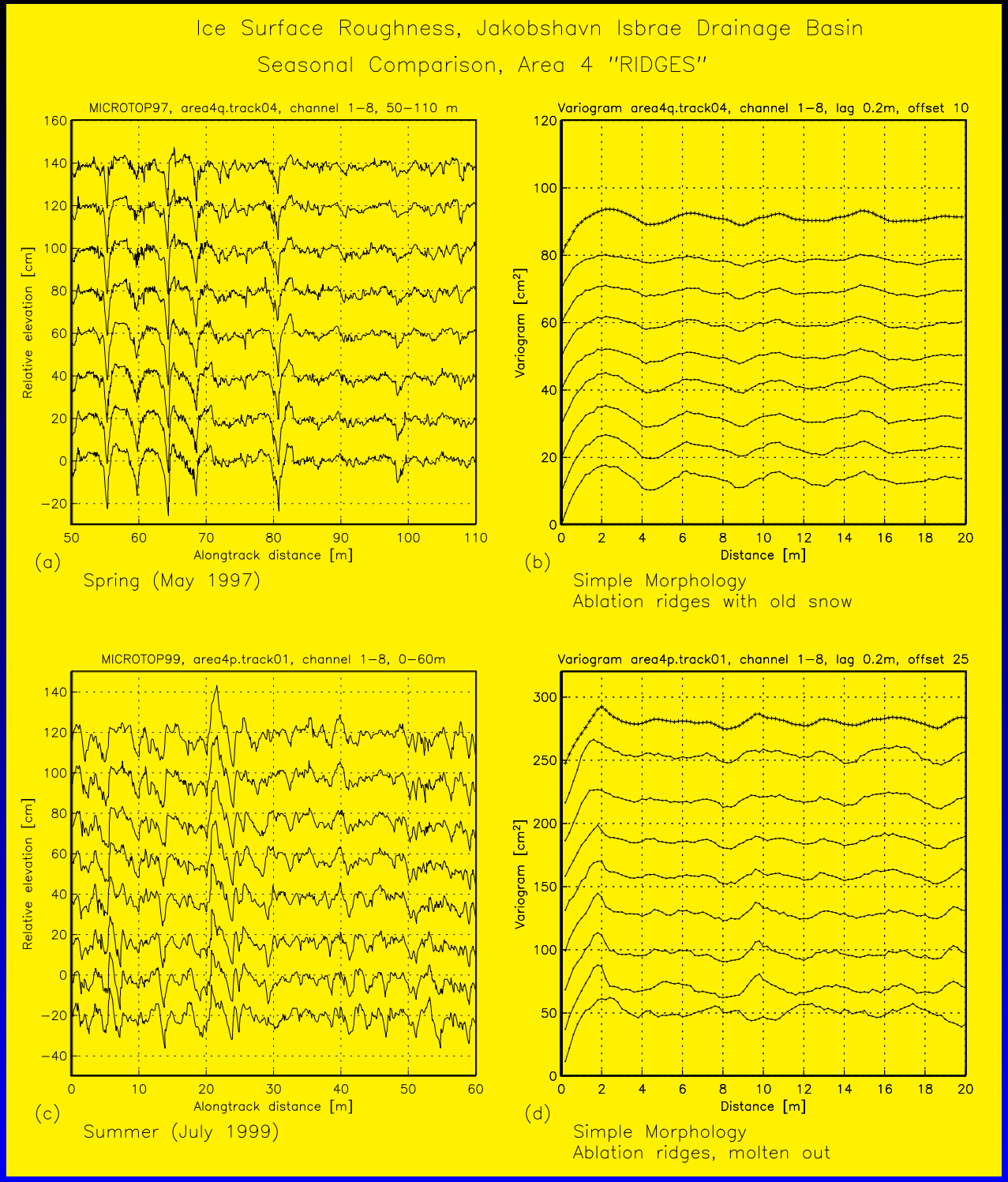
Ice Surface Roughness, Jakobshavn Isbrae Drainage Basin
Seasonal Comparison, Area 4 "RIDGES"
MICROTOP97, area4q.track04, channel 1–8, 50–110 m
Relative elevation [cm]
Alongtrack distance [m]
(a)
Spring (May 1997)
Variogram area4q.track04, channel 1–8, lag 0.2m, offset 10
Variogram [cm²]
Distance [m]
(b)
Simple Morphology
Ablation ridges with old snow
MICROTOP99, area4p.track01, channel 1–8, 0–60m
Relative elevation [cm]
Alongtrack distance [m]
(c)
Summer (July 1999)
Variogram area4p.track01, channel 1–8, lag 0.2m, offset 25
Variogram [cm²]
Distance [m]
(d)
Simple Morphology
Ablation ridges, molten out

Parameters for complex morphology

Define $p2$-type parameters $pt2(\cdot,\cdot)$ as

$$pt2(max_i, min_j) = \frac{\gamma_{max_i} - \gamma_{min_j}}{\gamma_{max_i}}$$

for $i \leq j$.
With this notation, we define significance parameters for the first few minima in the vario function:

$$p3 = pt2(max_1, min_2)$$

$$p4 = pt2(max_2, min_2)$$

$$p5 = pt2(max_s, min_2)$$

Feature vectors

Parameters are composed into *feature vectors*, on which the classification is based.

Selection of parameters depends on the applied problem.

Characteristic Snow Forms

Winter sastrugi	**Summer** sun cups
rougher	smoother
pond high	*pond* low
complexely shaped surface	regularly, evenly shaped surface
large size range of features	well-defined characteristic sizes
$min_a = 2$ m	$min_a = 0.4$-0.6 m $min_b = 2.2$-2.4 m $min_c = 7$ m
avgspac often not defined	*avgspac* well defined
deriv high	*deriv* low
narrow first *max* significant first *min*	$min - max$ sequence with regular multiples

An application of snow- and ice-surface-roughness studies:

(1) Derivation of mathematical relationship bt surface roughness and geostatistical characterization

(2) Calculation of surface roughness from GRS measurements

(3) Utilization of micrometeorological observations (PARCA Network Greenland; Mountain Research Station, Niwot Ridge)

(4) Calculation of energy available for melting (with J. Box, M.Kuhn)

Result: Melt energy varies by a factor of 2.6 dependent on surface roughness !!

MICROTOP 97 Team Boarding Sykorsky S61 in Illulissat

#1 (R:ASTER VNIR_Band3N,G:ASTER VNIR_Band2,B:ASTER VNIR_Band1):ast_l1tjak.hdf

File Overlay Enhance Tools Window

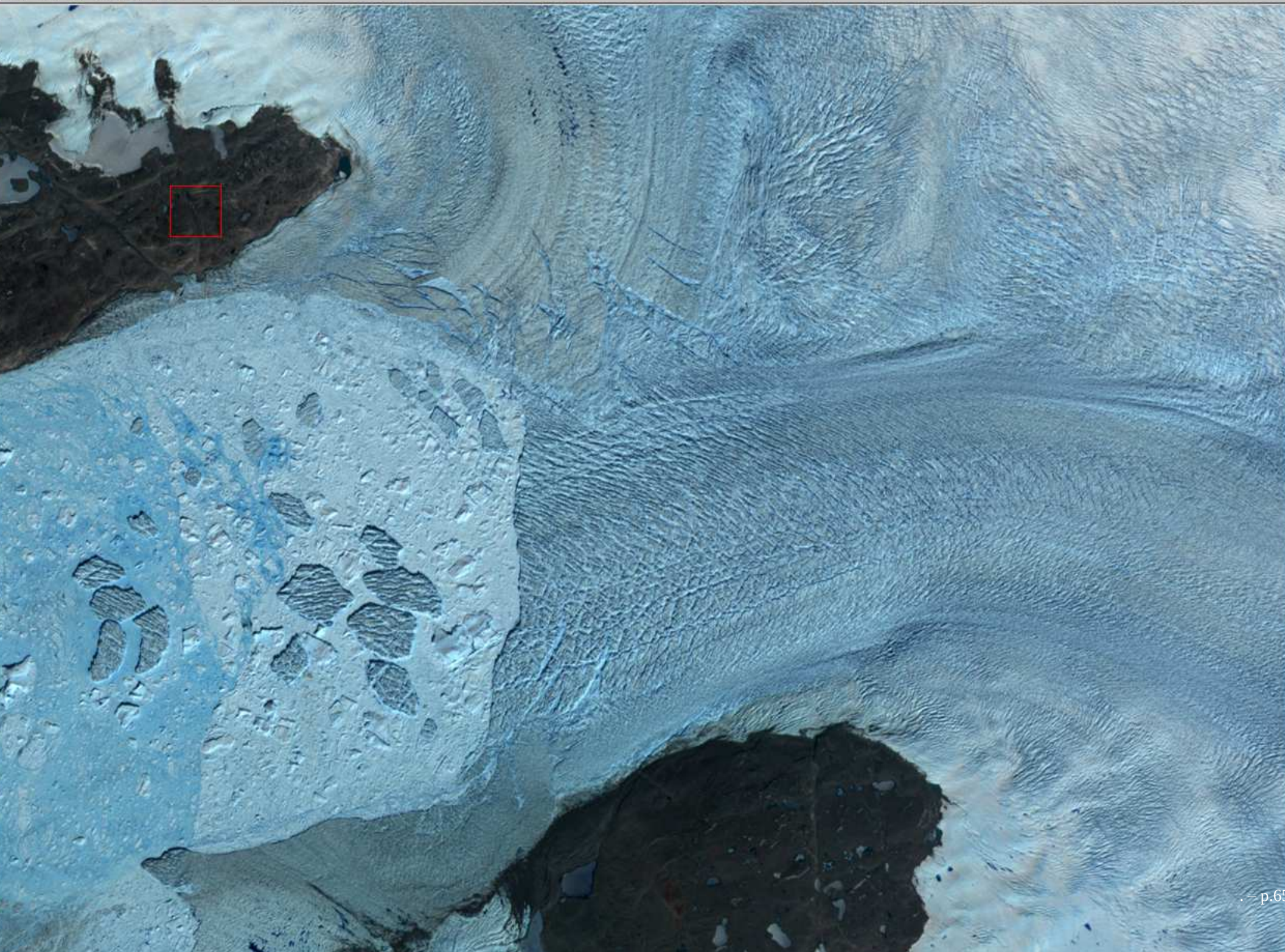

File Overlay Enhance Tools Window

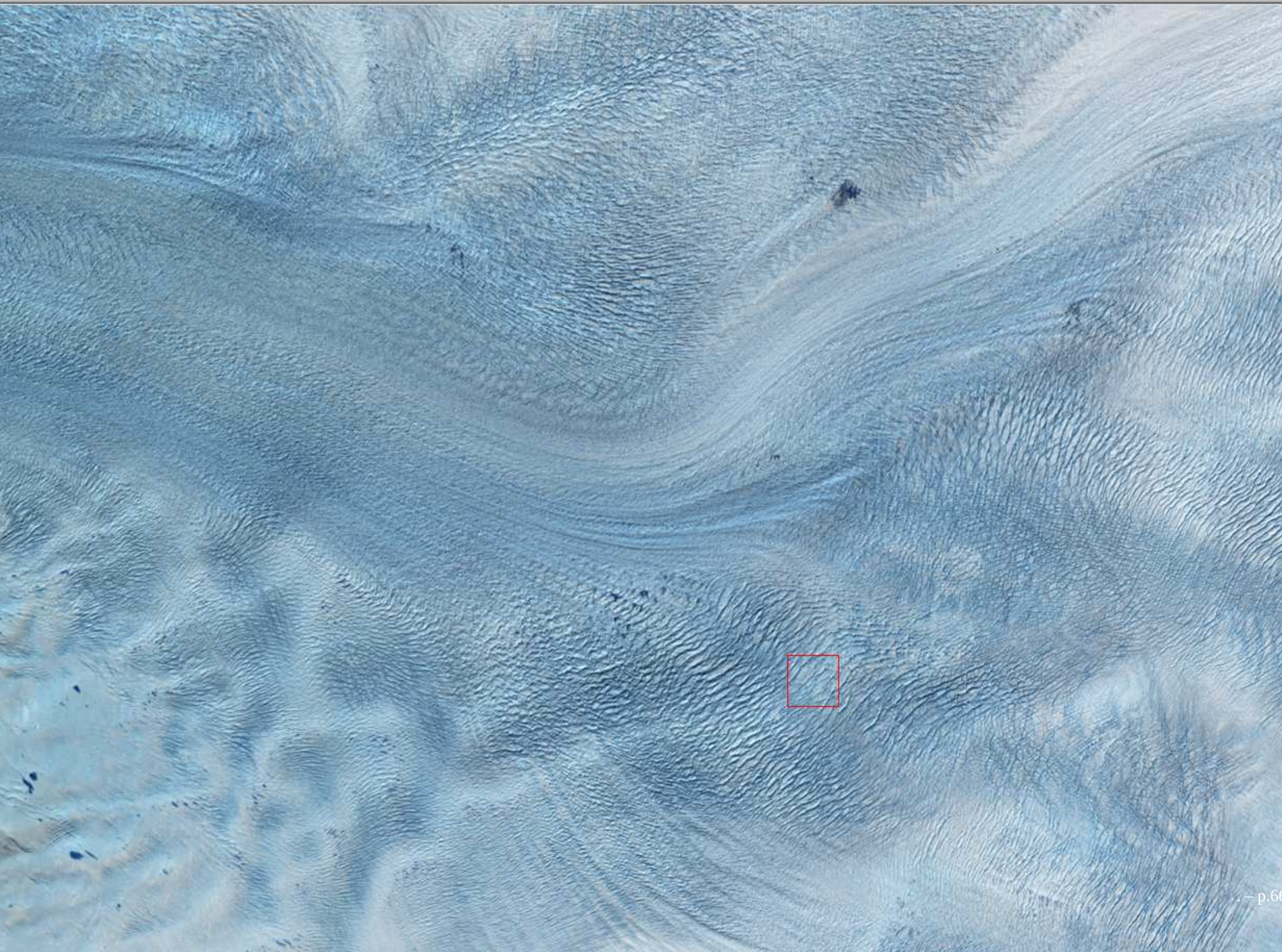

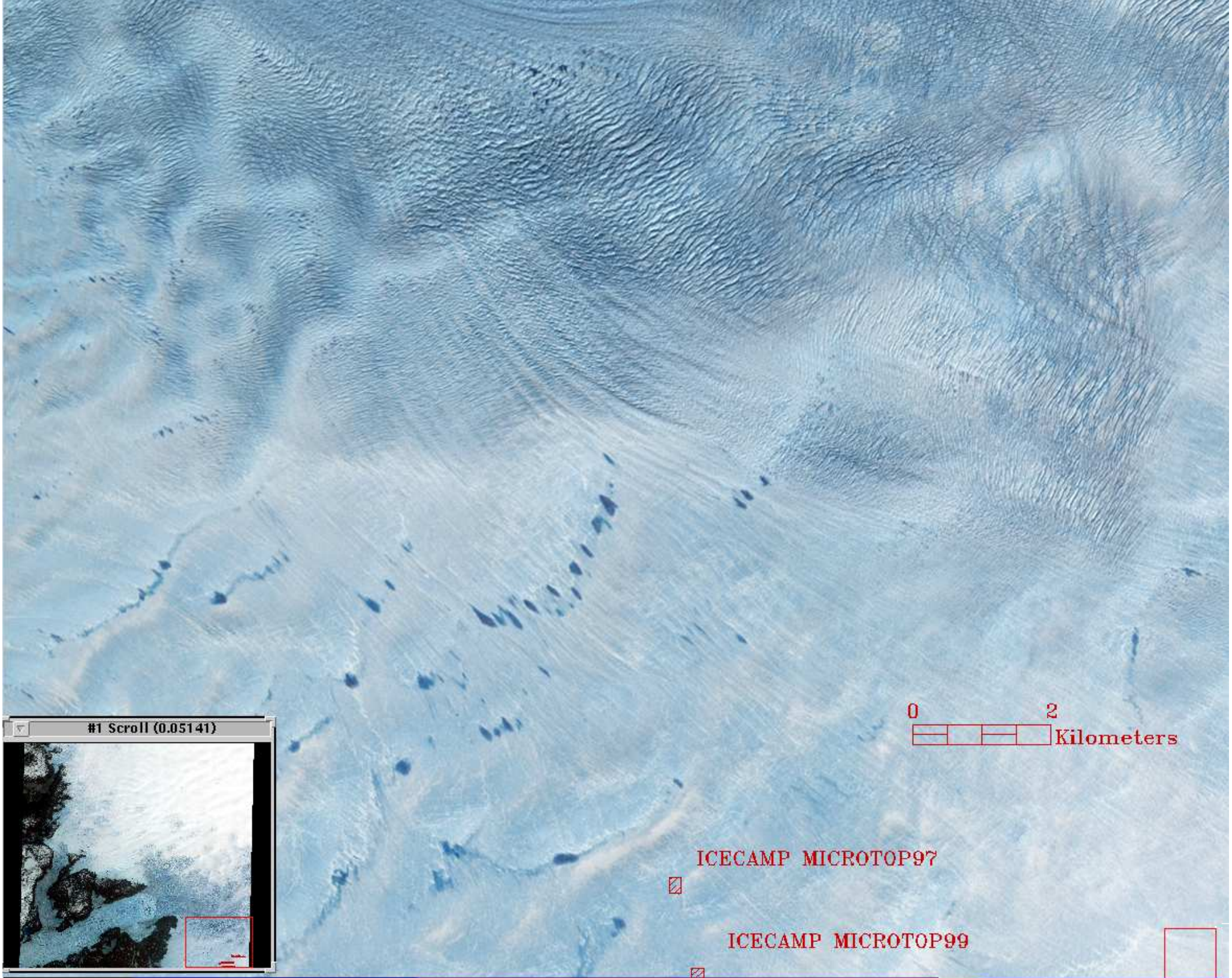
#1 Scroll (0.05141)
0
2
Kilometers
ICECAMP MICROTOP97
ICECAMP MICROTOP99

Jakobshavns Isbræ: Calving Front, July 2005

Mapping Deformation Properties using Geostatistical Classification based on ASTER DATA

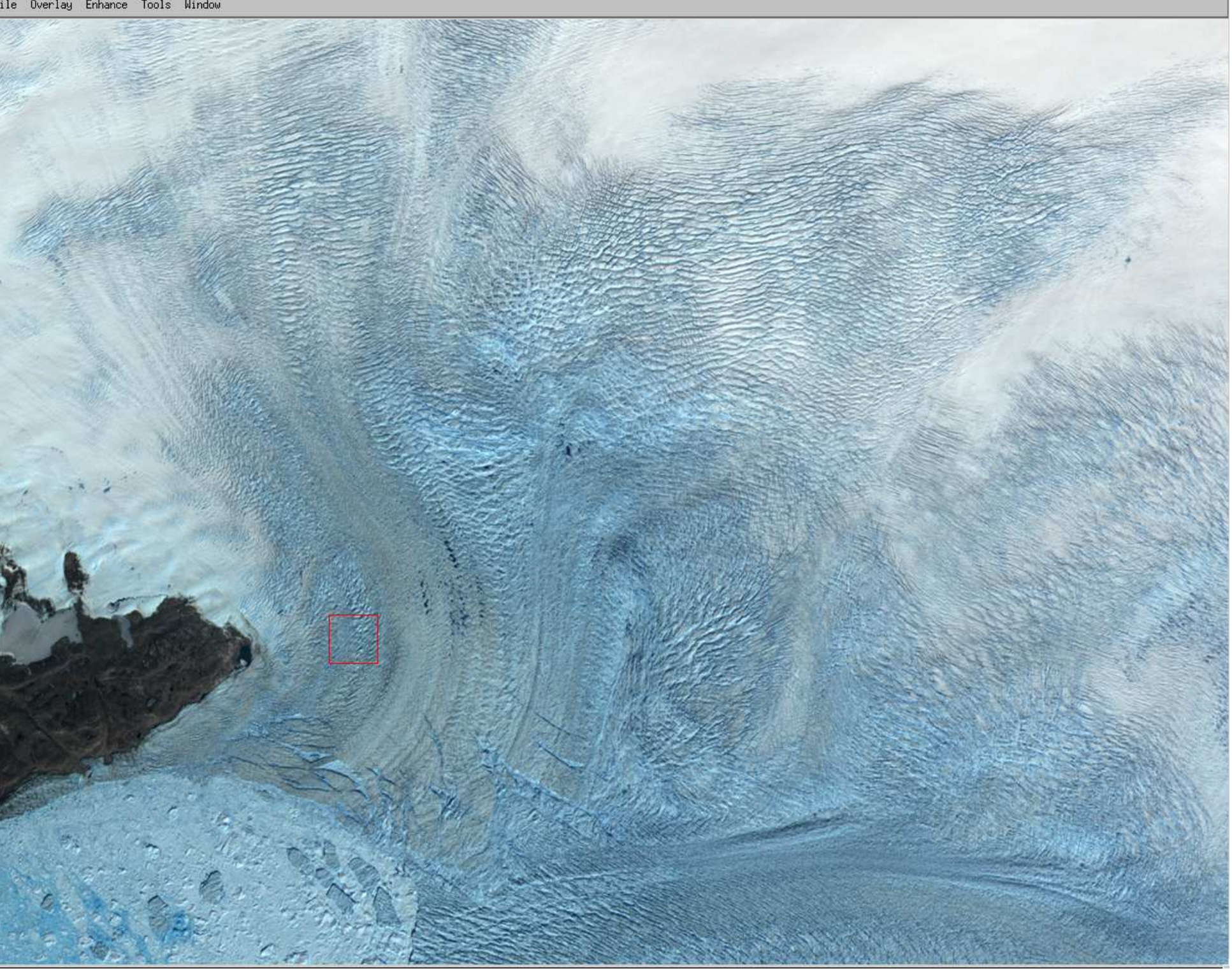

Jakobshavns Isbræ: North Icestream — ASTER Data, May 2003

ASTER Data Classification: Parameter *pond*

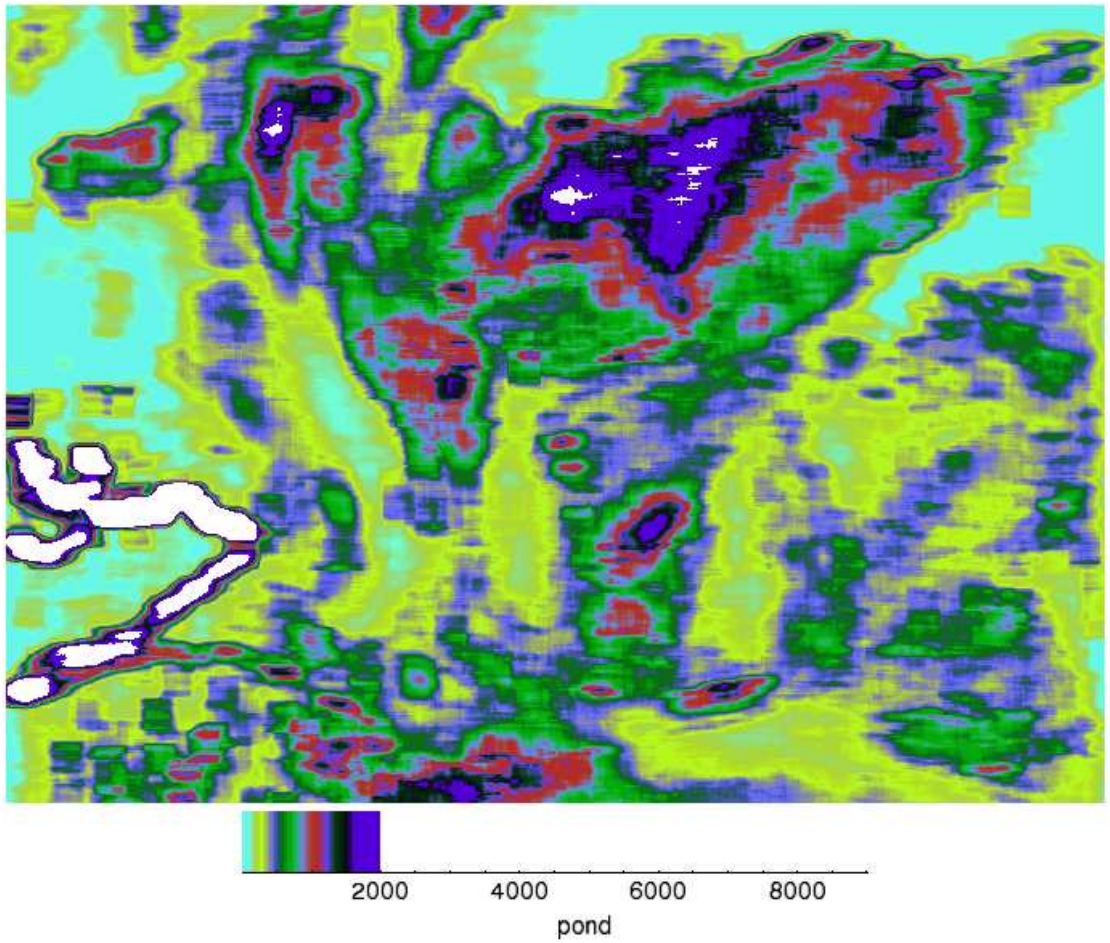

ASTER Data Classification: Parameter $p1$

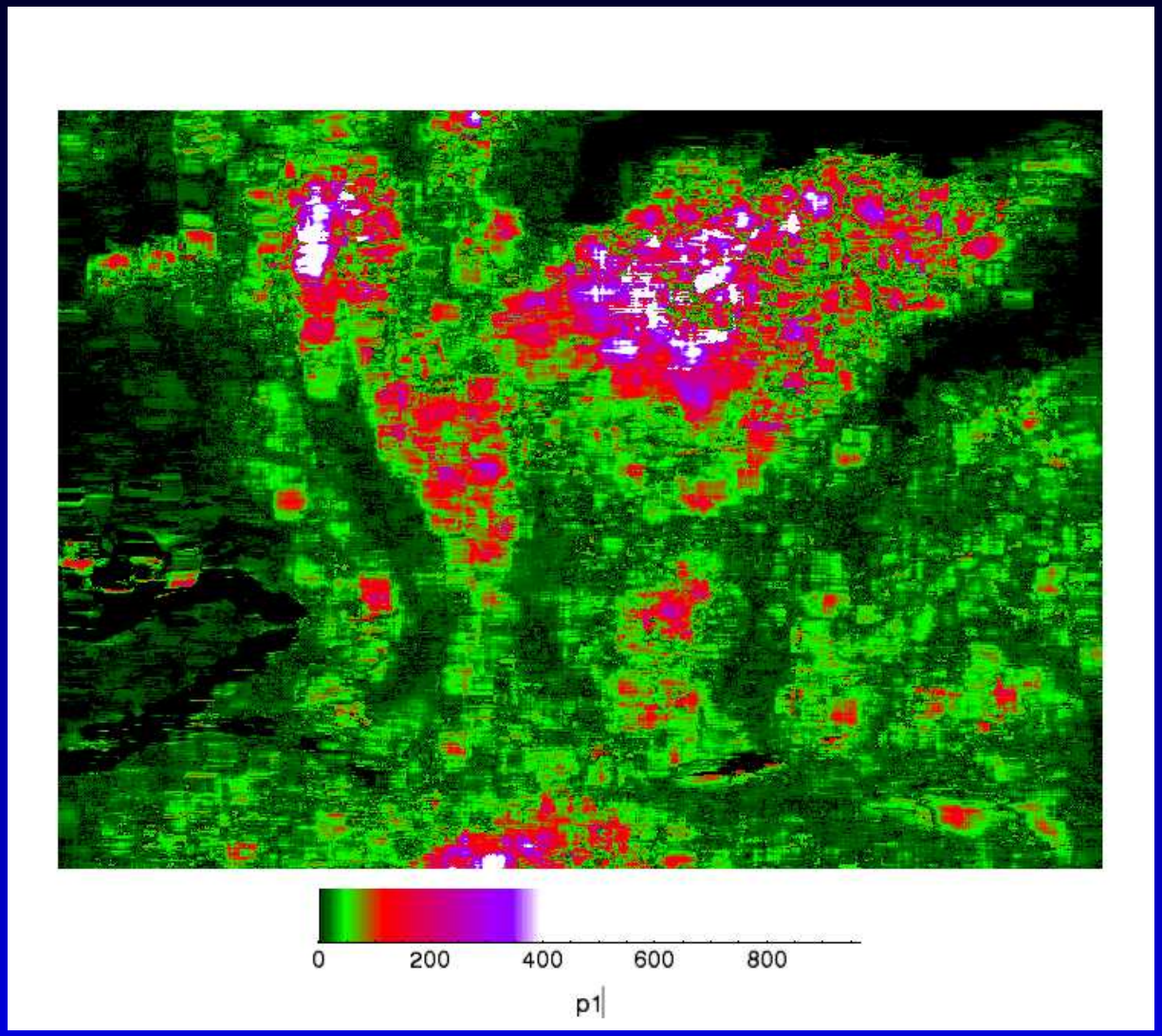

window 20, offset 1, direction N-S

ASTER Data Classification: Parameter $p2$

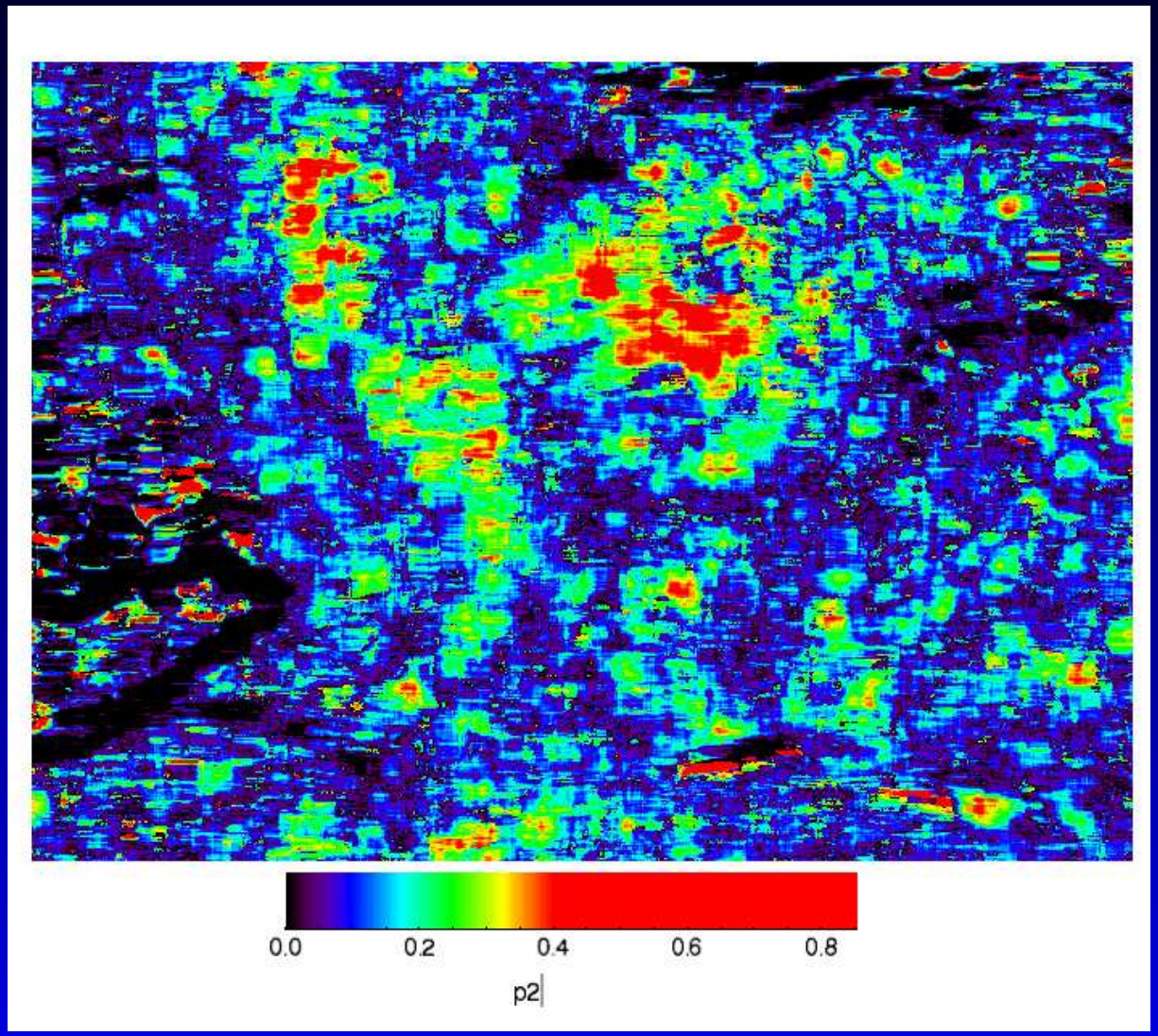

window 20, offset 1, direction N-S

Applications

- Monitor changes in front position (retreat!)
- Study morphogenetic processes (eg. location of melt features)
- Map deformation states and kinematic provinces
- Notice changes in ice-dynamic processes

Sea Ice in the Alaskan Arctic

Characterization and Segmentation
of Sea-Ice Provinces
Using Hyperparameters
in Geostatistical Classification

Beaufort Sea, Ridge (March 2003) (J. Maslanik photo)

Rubbled Ice (March 2003) (J. Maslanik photo)

Snow-depth surveying on sea-ice ridge (March 2003)

(J. Maslanik photo)

Snow on Sea Ice
Depth Profiles: Beaufort Sea

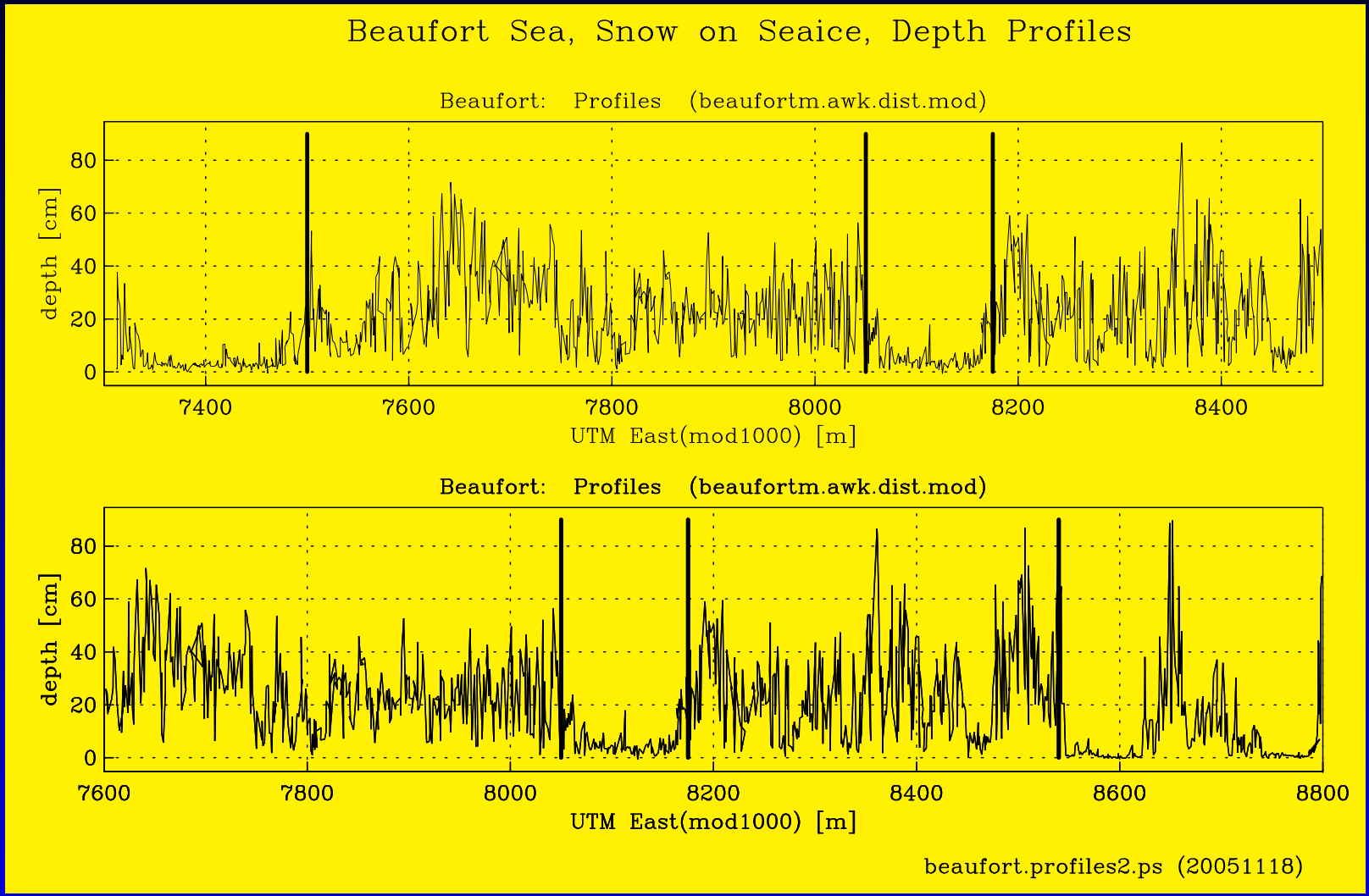

Snow on Sea Ice
Depth Profiles: Elson Lagoon

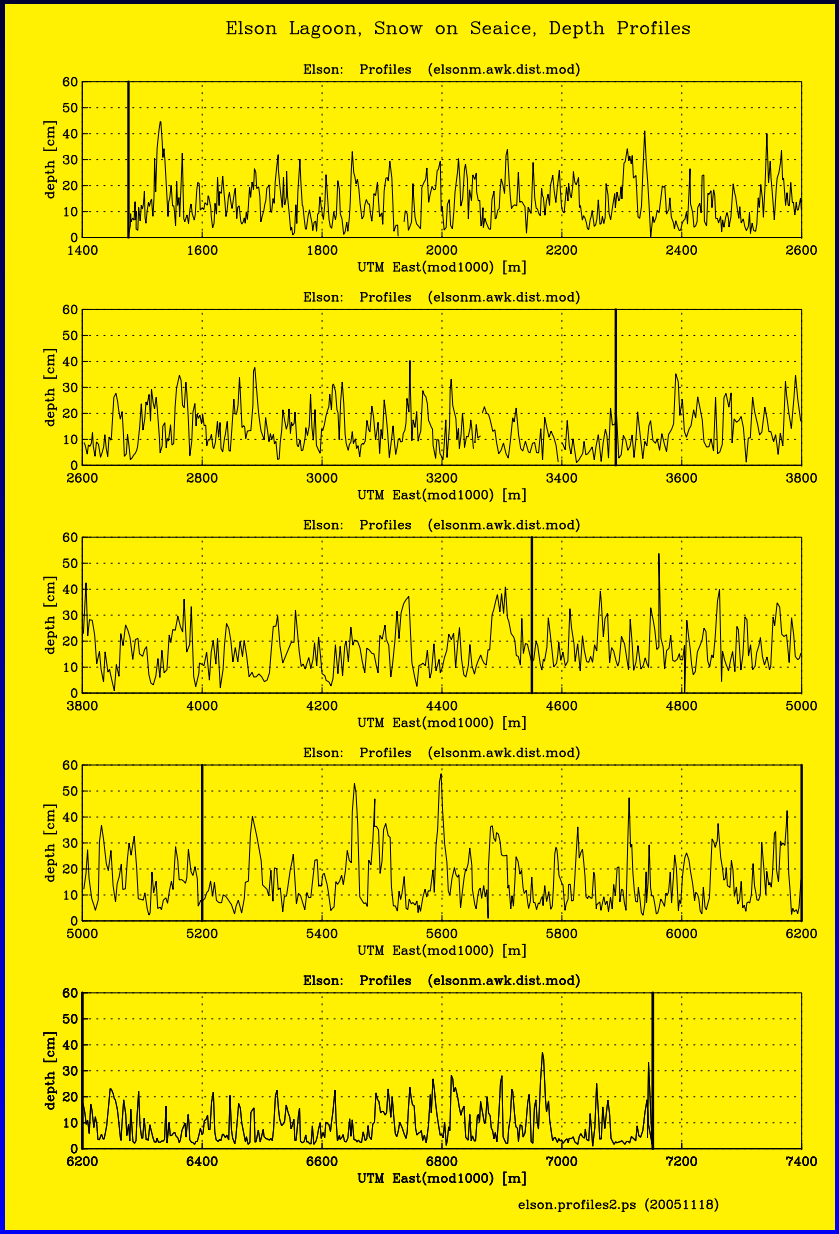

Snow on Sea Ice
1st-Order Vario Functions

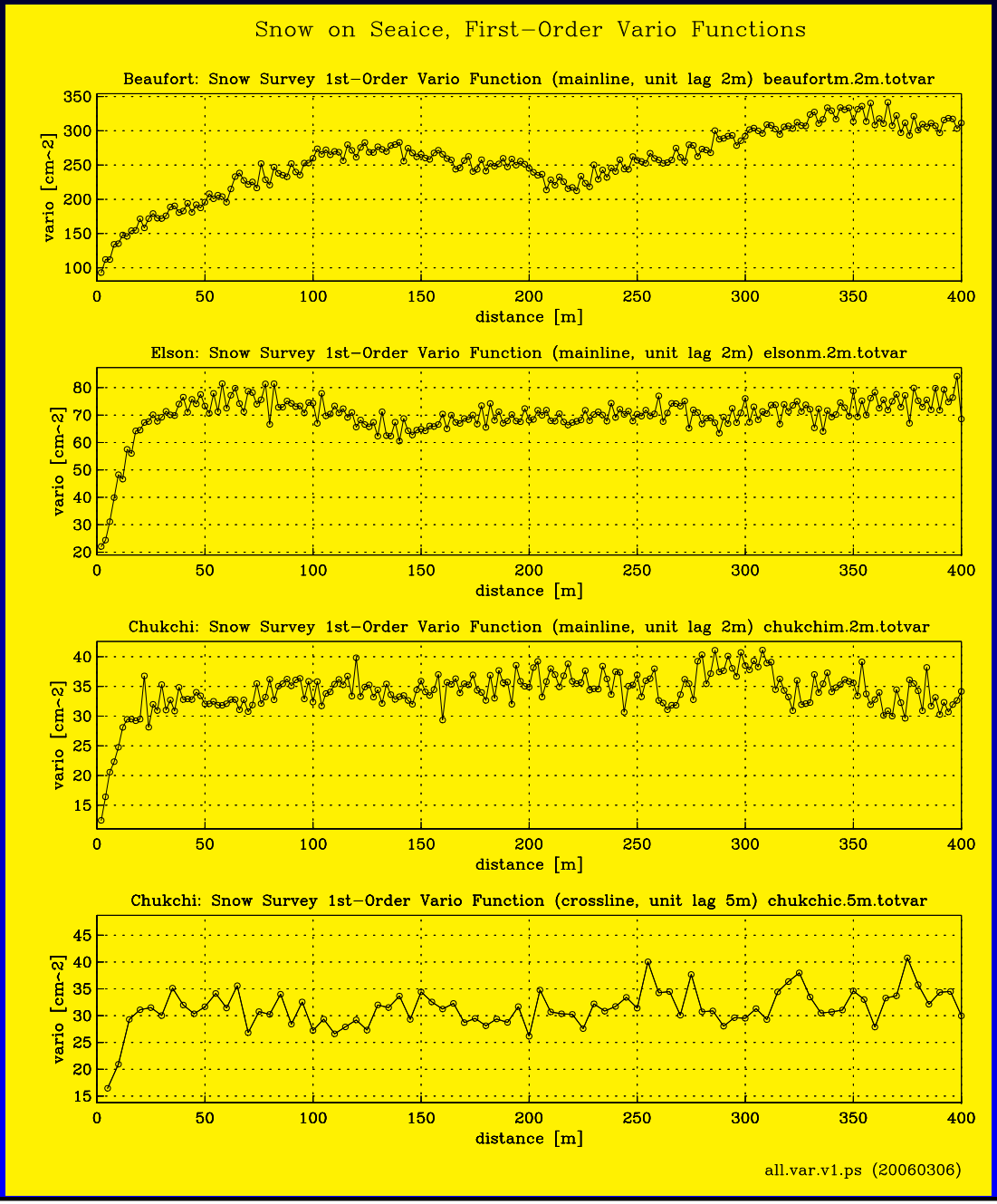

Beaufort Sea

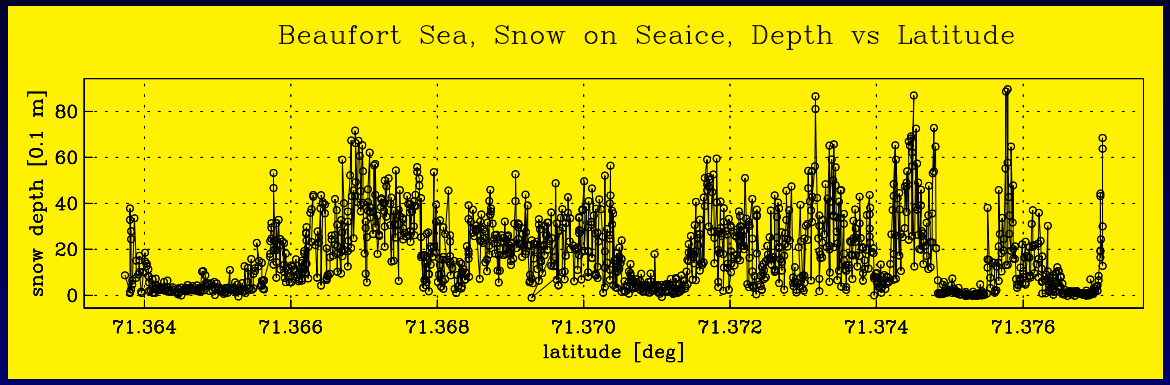

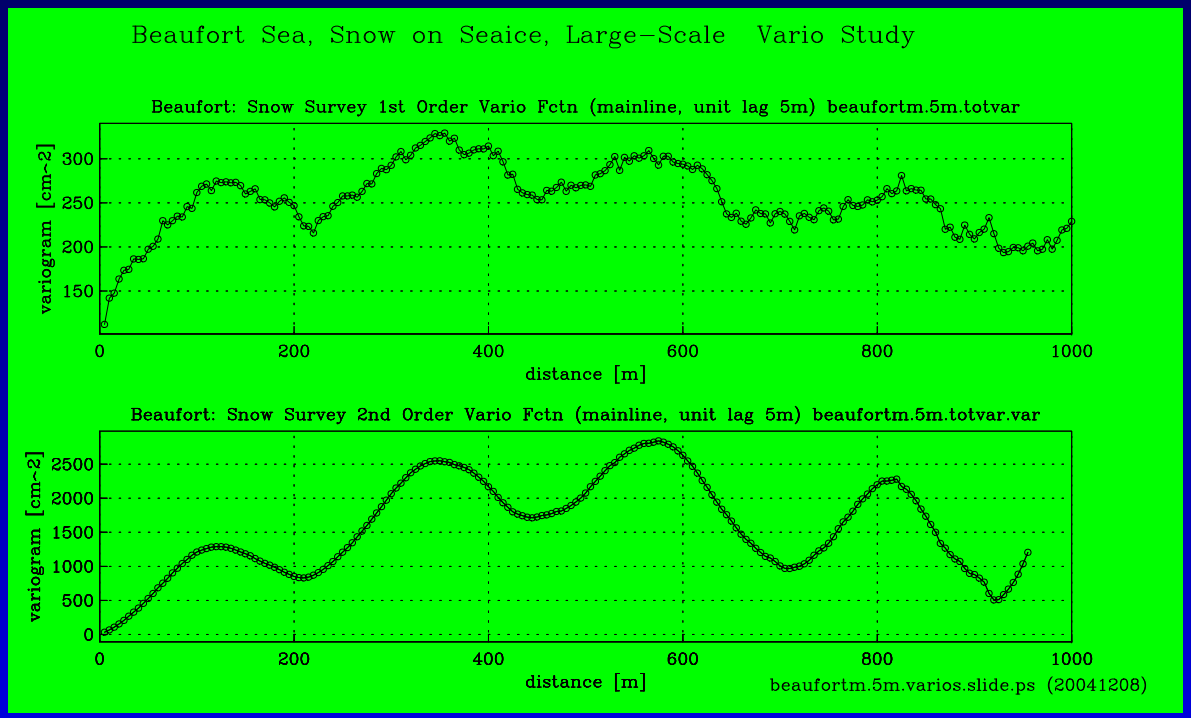

parameter type $pt1(max_i, min_j)$

	min_1	min_2	min_3	min_4
max_1	+0.27	+0.04	+0.10	+0.04
max_2		+0.20	+0.18	+0.07
max_3			+0.43	+0.08
max_4				+0.42

parameter type $pt2(max_i, min_j)$

	min_1	min_2	min_3	min_4
max_1	+0.05	+0.03	+0.11	+0.10
max_2		+0.07	+0.15	+0.13
max_3			+0.14	+0.13
max_4				+0.19

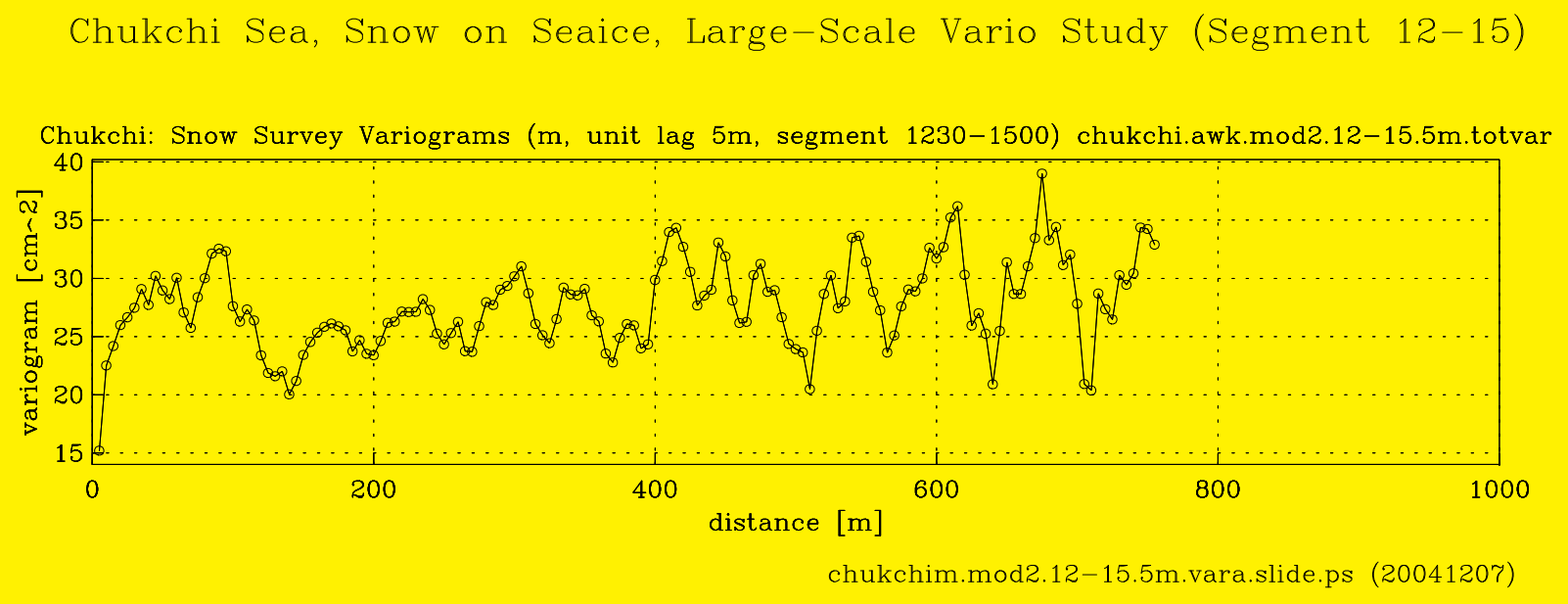

		min						pt2			pt1			
File	mindist	2	3	4	pond	p1	p2	p3	p4	p5	p6	p7	p8	p9
beaufortm.5m.totvar.var	210	445	710	920	4873	5.4	0.356	-0.328	0.328	0.328	-1.3	8.8	8.8	0.659
beaufort.awk.75-81.5m.totvar.var	25	35	60	75	11195	5.0	0.092	-0.155	0.114	0.114	-2.8	8.2	8.2	0.087
beaufort.awk.82-85.5m.totvar.var	50	60	80	90	116795	117.4	0.511	0.496	0.061	0.496	81.4	37.6	81.4	0.021
elsonm.5m.totvar.var	70	85	95	140	779	0.0	0.004	0.029	0.031	0.031	0.0	0.1	0.1	0.024
elson.awk.14-35.5m.totvar.var	90	120	130	190	361	0.4	0.223	0.134	0.038	0.134	0.1	0.3	0.1	0.011
elson.awk.35-46.5m.totvar.var	125	260	405	535	668	2.7	0.654	0.776	0.767	0.776	1.0	2.4	1.0	0.513
elson.awk.46-52.5m.totvar.var	30	45	55	65	850	2.1	0.077	0.057	0.037	0.057	0.4	1.0	0.4	0.042
elson.awk.52-62.5m.totvar.var	80	95	130	145	2094	1.6	0.176	0.171	0.017	0.171	1.0	0.8	1.0	0.320
elson.awk.62-74.5m.totvar.var	55	85	120	135	81	0.0	0.038	-0.040	0.073	0.073	-0.0	0.3	0.3	0.393
chukchim.5m.totvar.var	30	45	65	100	137	0.0	0.015	-0.003	0.005	0.005	-0.0	0.0	0.0	0.099
chukchim.mod1.5m.totvar.var	25	35	90	100	87	0.0	0.026	-0.029	0.036	0.036	-0.0	0.1	0.1	0.014
chukchim.mod2.5m.totvar.var	30	60	90	100	227	0.0	0.019	0.077	0.146	0.146	0.0	0.1	0.1	0.051
chukchi.awk.mod2.12-15.5m.totvar.var	145	200	260	340	273	0.8	0.335	0.436	0.183	0.436	0.5	0.3	0.5	0.083
chukchic.5m.totvar.var	45	65	80	100	163	0.3	0.131	0.109	0.122	0.122	0.1	0.5	0.5	0.033
beaufortm.2m.totvar.var	124	132	140	152	21090	12.8	0.012	0.013	0.010	0.013	2.8	3.7	2.8	0.038
beaufort.awk.75-81.2m.totvar.var	12	24	28	36	4277	0.6	0.015	-0.348	0.023	0.023	-3.6	2.6	2.6	0.003
beaufort.awk.82-85.2m.totvar.var	14	28	32	38	31824	16.7	0.033	-0.472	0.022	0.022	-29.4	16.8	16.8	0.063
elsonm.2m.totvar.var	28	40	44	50	1452	0.1	0.006	-0.185	0.037	0.037	-0.5	0.4	0.4	0.045
elson.awk.14-35.2m.totvar.var	28	38	46	50	1231	0.0	0.001	-0.064	0.041	0.041	-0.2	1.0	1.0	0.009
elson.awk.35-46.2m.totvar.var	12	16	34	44	1026	5.0	0.173	-0.054	0.015	0.015	-0.8	0.9	0.9	0.065
elson.awk.46-52.2m.totvar.var	10	16	24	28	1266	25.1	0.238	0.027	0.027	0.027	0.7	2.8	0.7	0.069
elson.awk.52-62.2m.totvar.var	8	14	18	24	5912	-17.3	0.285	0.119	0.274	0.274	14.5	-40.5	-40.5	0.169
elson.awk.62-74.2m.totvar.var	8	14	18	22	299	-1.9	0.304	0.141	0.248	0.248	1.7	-3.5	-3.5	0.308
chukchim.2m.totvar.var	8	14	22	30	181	-0.7	0.397	0.018	0.203	0.203	0.1	-0.3	-0.3	0.181
chukchim.mod2.2m.totvar.var	8	16	22	30	214	-1.3	0.481	0.117	0.255	0.255	0.3	-0.8	-0.8	0.249
chukchi.awk.mod2.12-15.2m.totvar.var	30	34	40	46	167	0.0	0.008	-0.014	0.002	0.002	-0.0	0.0	0.0	0.071
beaufortm.totvar.var	5	8	21	23	12868	27.3	0.157	-0.148	0.098	0.098	-6.4	21.5	21.5	0.001
beaufort.awk.75-81.1m.totvar.var	6	9	11	15	8650	25.2	0.078	0.078	0.026	0.078	6.3	3.9	6.3	0.187
beaufort.awk.82-85.1m.totvar.var	5	8	10	12	17112	243.8	0.222	-0.070	0.067	0.067	-19.1	84.6	84.6	0.250
elsonm.totvar.var	4	18	25	29	1187	-3.5	0.675	0.009	0.146	0.146	0.6	-1.9	-1.9	0.105
chukchim.totvar.var	4	6	8	12	291	-2.3	0.238	0.207	0.265	0.265	2.0	-2.8	-2.8	0.282
chukchim.mod2.1m.totvar.var	4	6	8	10	386	-5.6	0.278	0.350	0.318	0.350	7.1	-6.1	7.1	0.271
chukchi.awk.mod2.12-15.1m.totvar.var	6	8	10	12	94	0.1	0.008	-0.173	0.023	0.023	-0.6	0.3	0.3	0.026
chukchic.totvar.var	5	10	16	21	375	-37.5	0.582	0.485	0.489	0.489	46.8	-31.7	-31.7	0.336

Elson Lagoon Profile: varvar functions

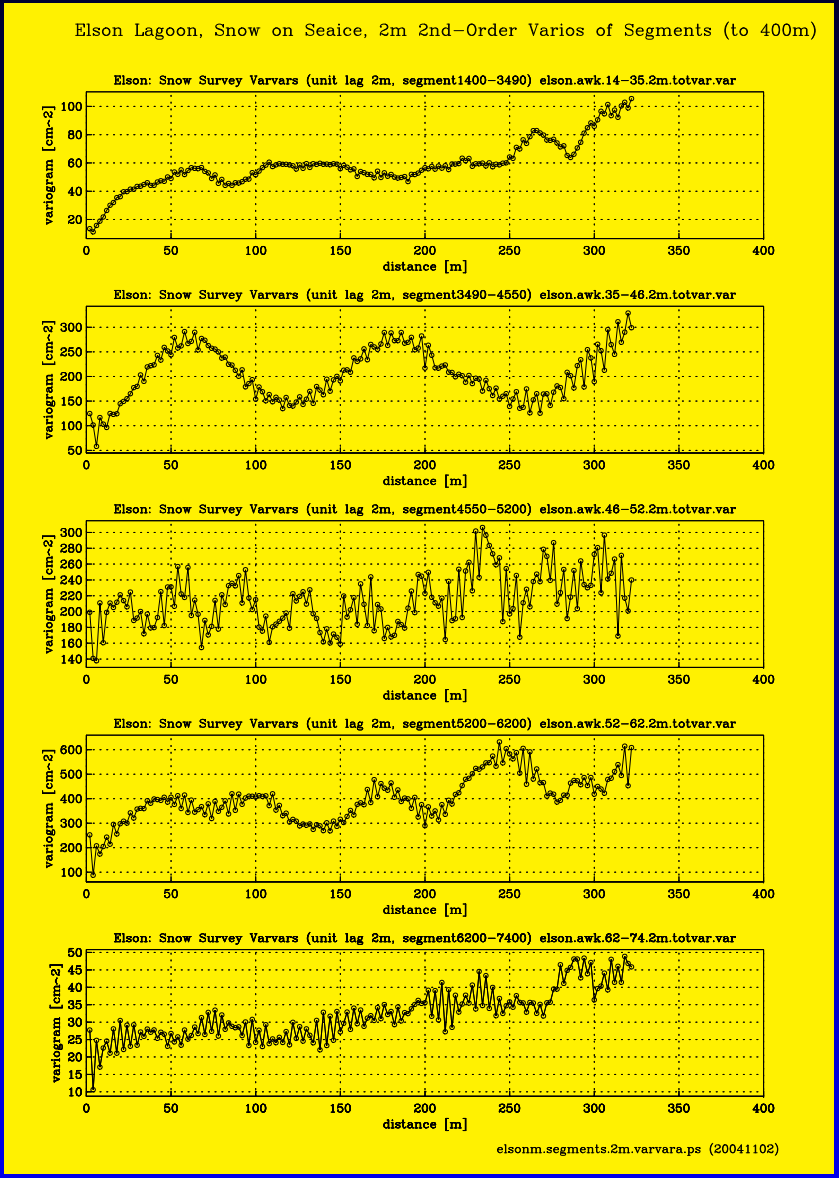

Robust search for hyperparams in complex geo-data sets

Determine *bigmax*, the largest maximum in a group of g maxima:

$$\gamma_{bigmax} = \max\{\gamma_{max_1}, \ldots, \gamma_{max_g}\}$$

say, $\gamma_{bigmax} = gamma_{max_k}$, some $k \epsilon \{1, \ldots, g\}$

$$h_{bigmax} = h_{max_k}$$

Then determine *bigmin*, the smallest minimum in a group of g minima following *bigmax*:

$$\gamma_{bigmin} = \min\{\gamma_{min_k}, \ldots, \gamma_{min_{k+g-1}}\}$$

say, $\gamma_{bigmin} = gamma_{min_r}$, some $r \epsilon \{k, \ldots, k+g-1\}$

$$h_{bigmin} = h_{max_r}$$

Important hyperparameters

Then:

$$pt1(bigmax, bigmin) = pt1(max_k, min_r)$$
$$pt2(bigmax, bigmin) = pt2(max_k, min_r)$$

Generalization: Determine all $bigmax_i$ and $bigmin_j$ analogously for a given groupsize g.

$$pt*(bigmax_i, bigmin_j) \quad \text{for} \quad * = 1, 2$$

Generalization: Determine the best groupsize automatically

Application to Sea Ice

Variable: Depth of snow on sea ice

– only first one or two bigmin-bigmax sequences needed

– group size can be large (>20)

Stability criterion for optimum groupsize:

$bigmax$-$bigmin$ pair remains for 3 consecutive groupsizes (take 1st one)

Applications of Hyperparameter Concept in Geostatistical Characterization

(1) A characterization of Arctic sea-ice provinces near Point Barrow

(2) Influence of spatial surface roughness on passive microwave data (PSR)

Segmentation of Elson Lagoon Profile

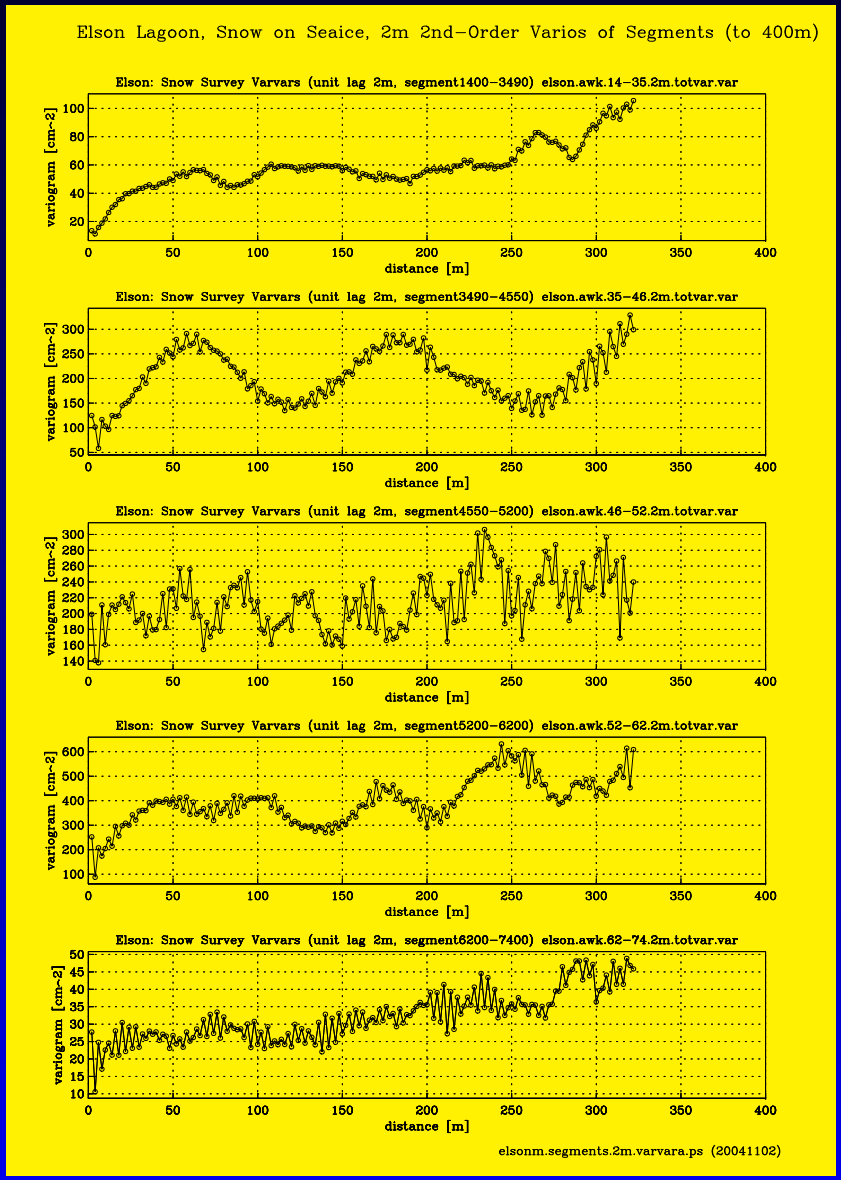

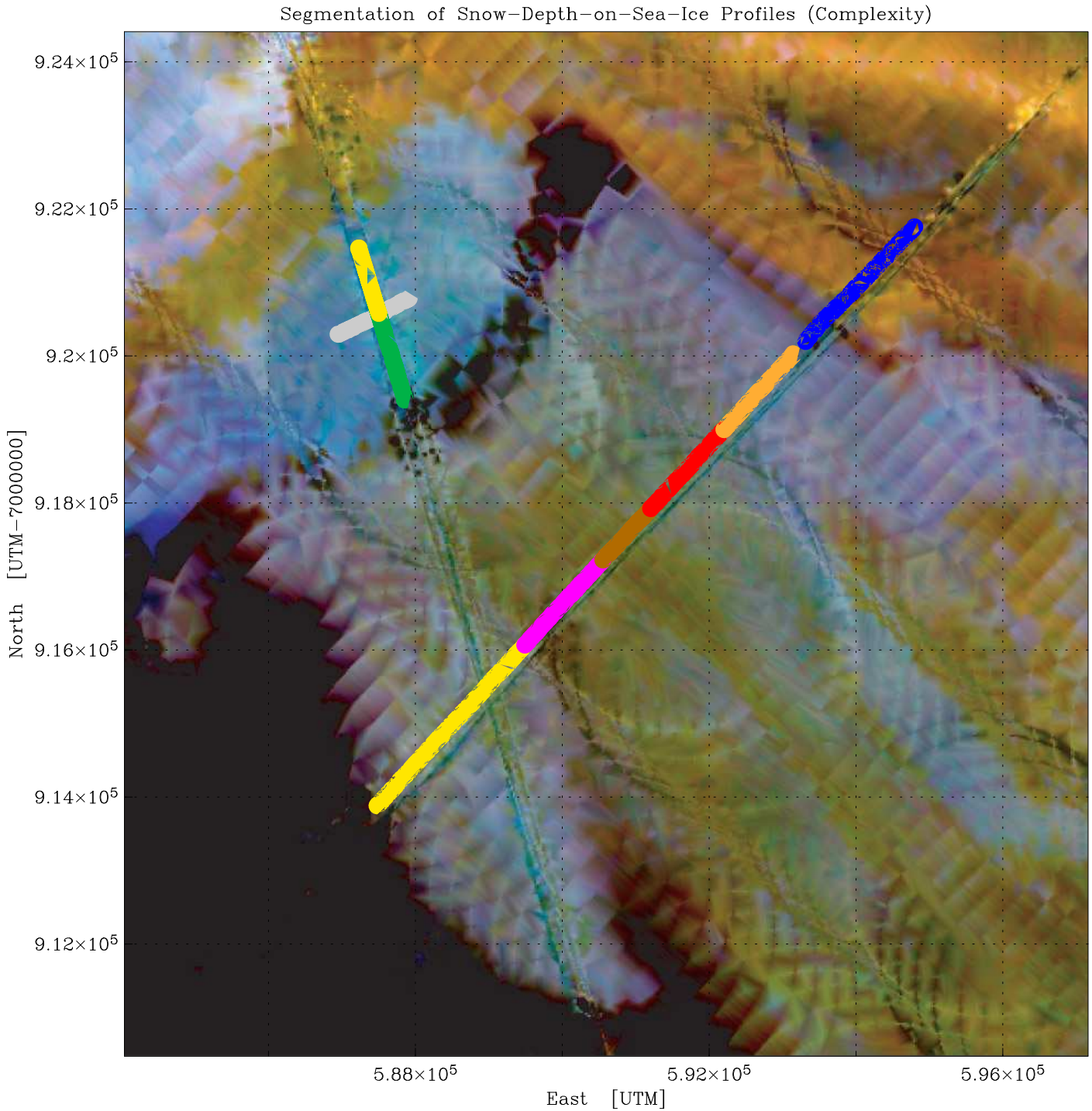

complexity of snow-depth structures: green-yellow-orange-brown-red-purple-green
PSR data: 10.7 GHz H-Pol (red), 19 GHz H-Pol (green), 37 GHz H-Pol (blue)

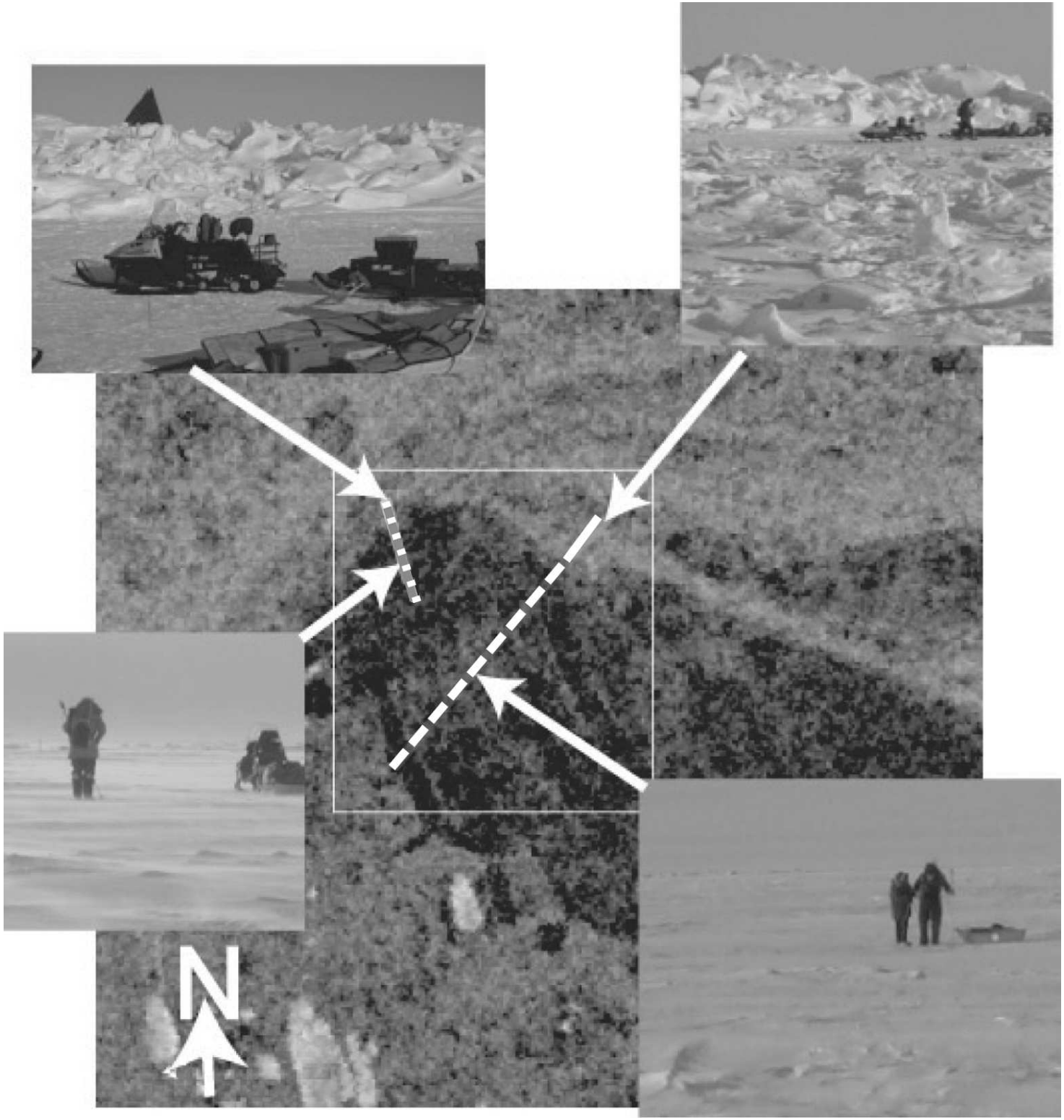
N

Conclusions

(1) Snow-depth on sea ice is an important indicator of sea-ice structure

(2) Complexity of spatial snow-depth structures is reflected in PSR data

(3) Snow-depth roughness length is less directly reflected in PSR data

(4) As surface roughness is approximated by snow-depth roughness, the above hold approximately (only) for surface roughness

Passive microwave data may be affected by snow-depth and surface roughness, with dependence on scale and quantified by geostatistical classification

Simulation of scale-dependent fractal fields

applied to derive measurement requirements for ICESat-2

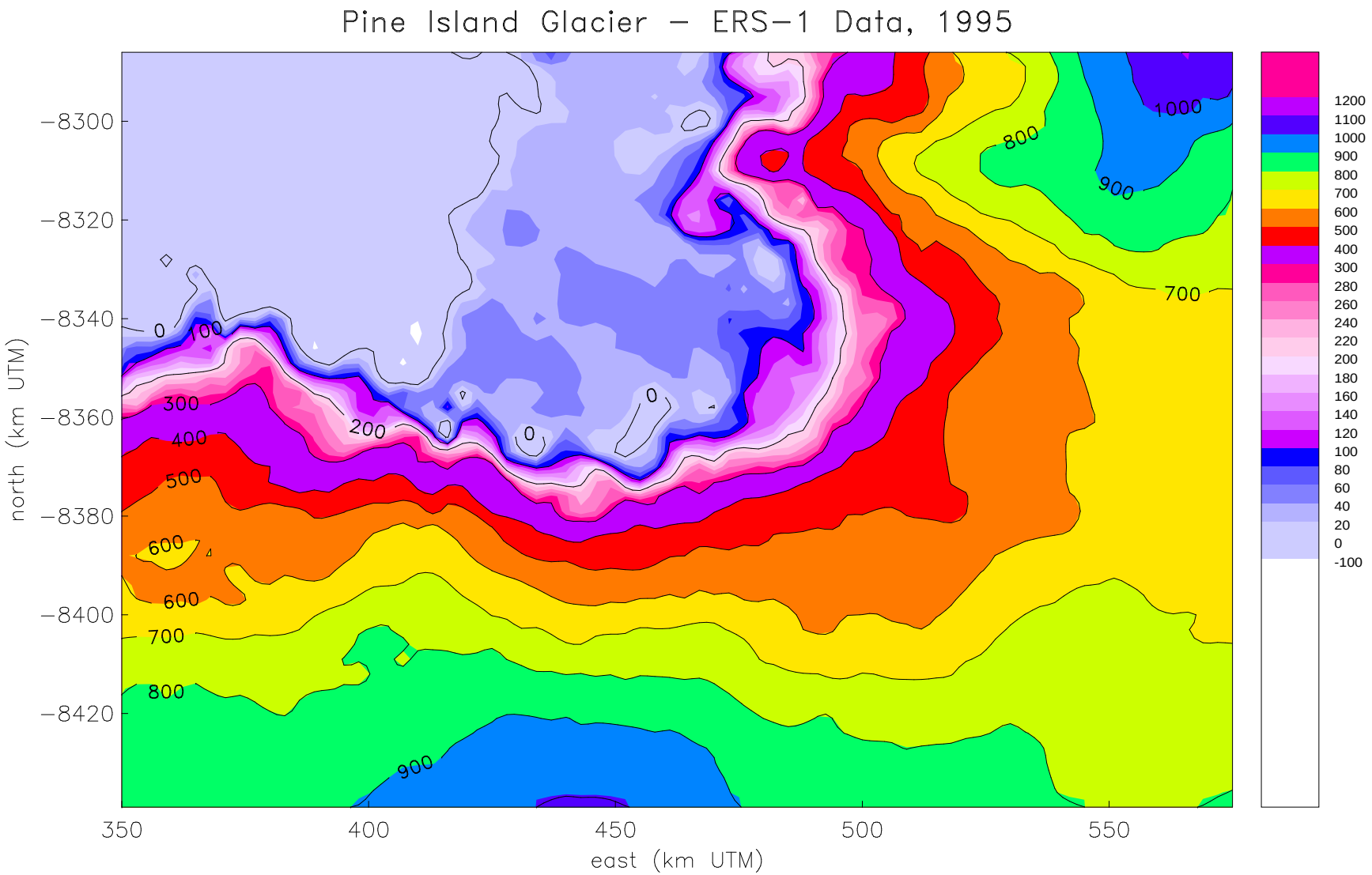

1:2000000, m261e243–279n71–77.e.smallpine2.v2.col8

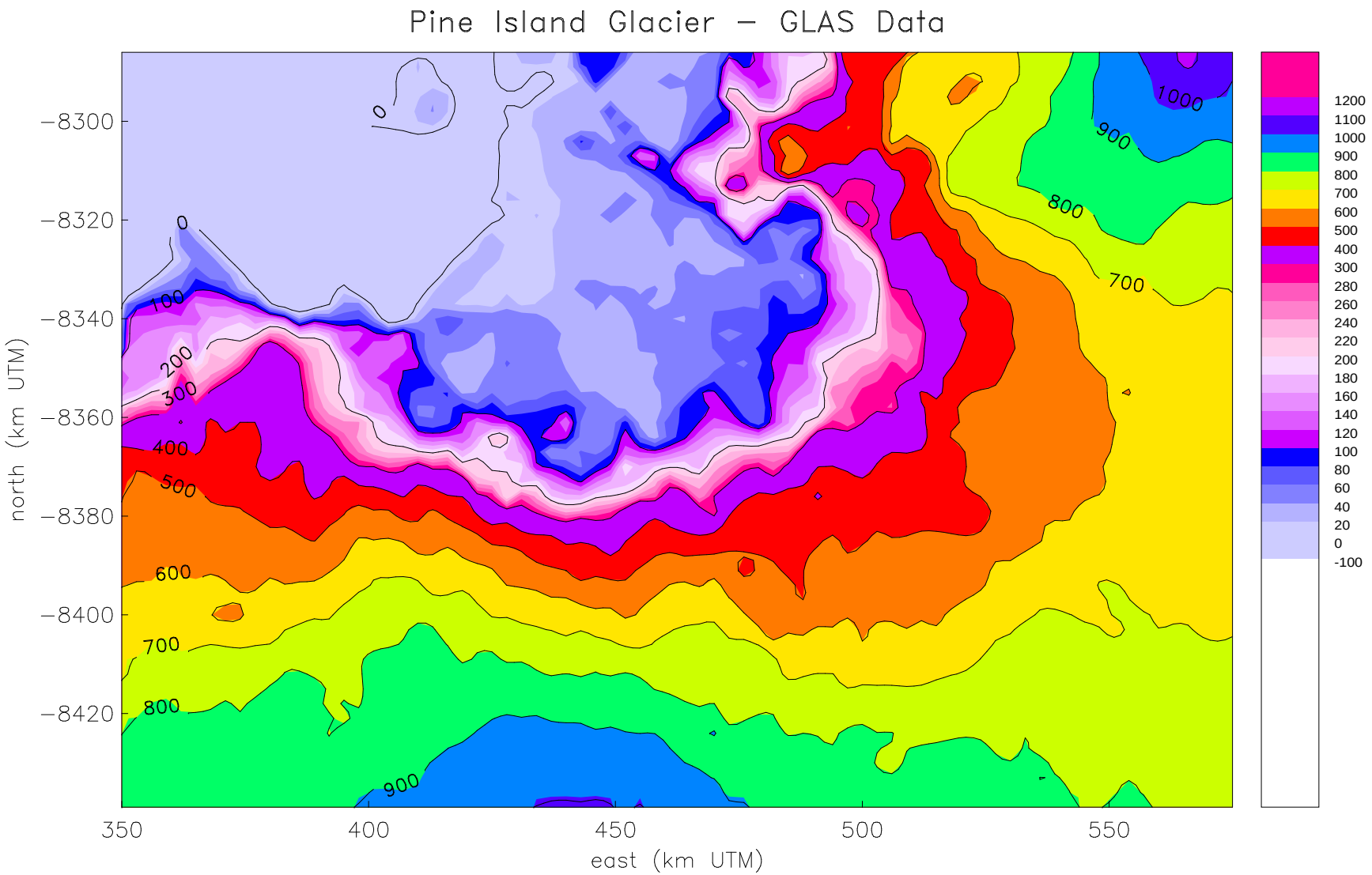

GLA06 Data, (Laser 2A, gain−crit, rel18), Oct/Nov 2003, vario(350,3450,6000m), search−rg 30km, 1:2000000, gla06.1.gain.smallpine2.v2.col8

Pine Island Glacier – GLAS (2003) minus ERS–1 (1995) [with ERS–1 contours]

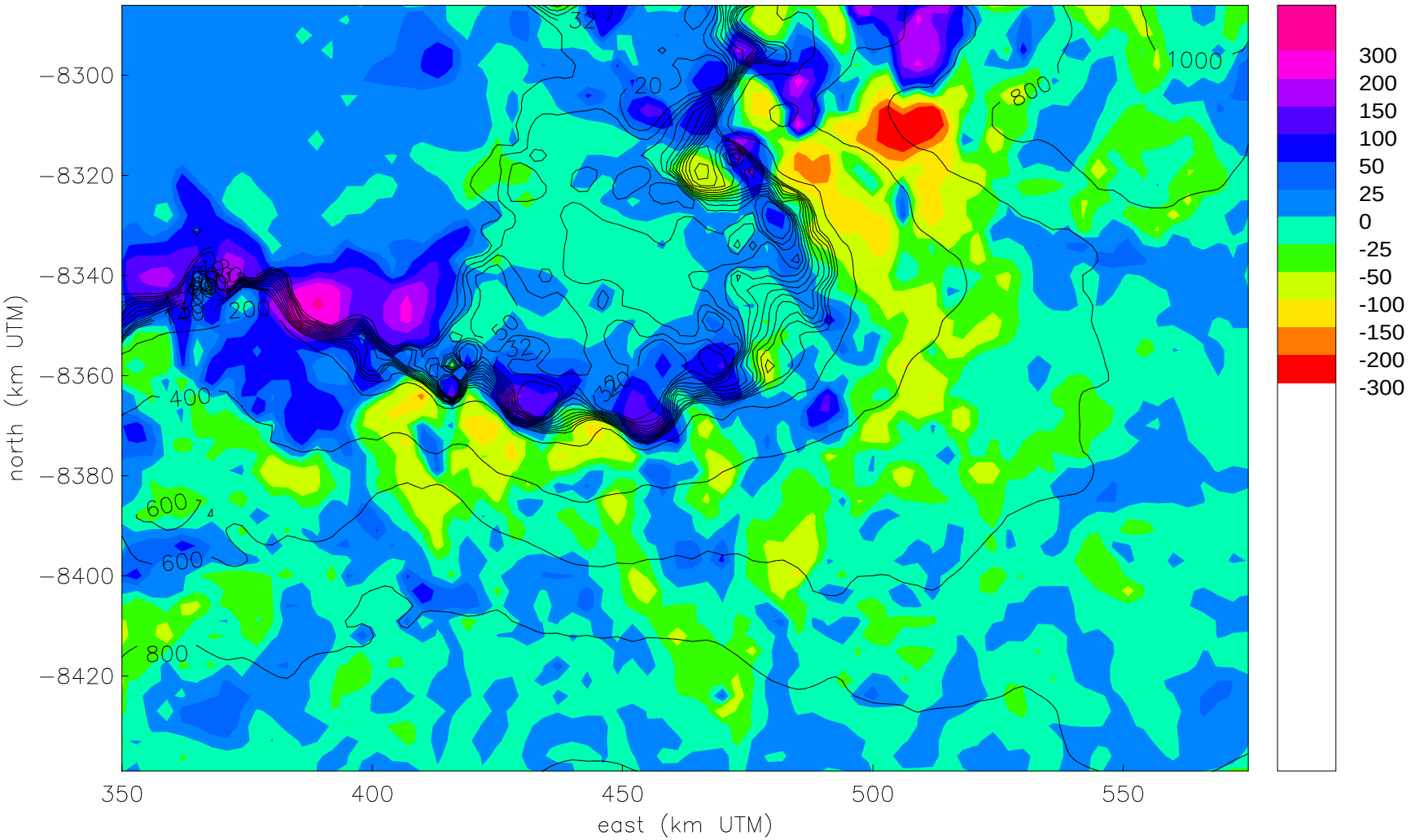

scale 1:2000000 diff glasgain–ers1.wers1cont.smallpine2.col10.v2.totps 20050404

gla06.1.gain.smallpine2.0.dtm minus m261e243–279n71–77.e.smallpine2.0.dtm

Role of Surface Roughness

To assess the potential of a multi-beam channel to measure high-resolution topography, we need information on spatial subscale roughness (ice surface roughness at a resolution higher than that of GLAS observations).

What is spatial surface roughness?

- a derivative of (micro)topography

$\longrightarrow$ characterization of spatial behavior

GRS Data – Roughness Model

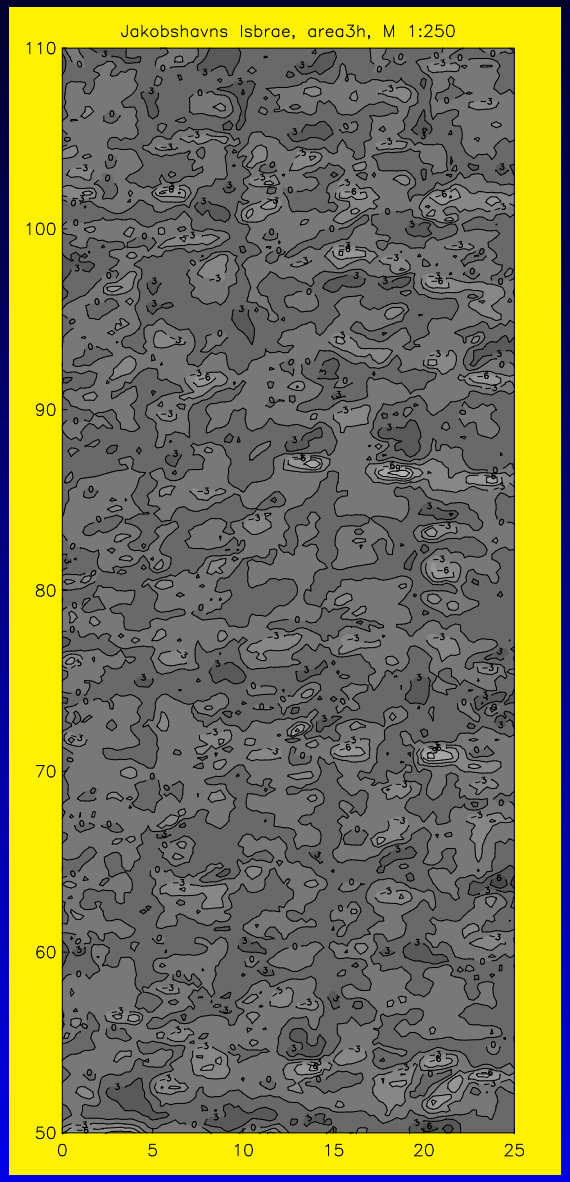

GRS Data

- data in 8 or 16 channels with across-track resolution 0.2 m
- along-track resolution ≈0.1 m
- subcentimeter vertical accuracy

DEMs from GRS data

- 0.2m grids
- areas typically 25 m by 200 m to 200 m by 200 m

Approach: Conditional Simulation of Ice Surfaces

(1) Use GLAS DEMs as low-res boundary conditions

(2) Use GRS data (from Greenland) to derive spatial surface roughness parameters using vario functions

(3) Derive SIMSURF model parameters:

- (a) scale breaks and their resolutions
- (b) at every scale range:
  - (b.1) fractal dimension
  - (b.2) direction of anisotropy
  - (b.3) anisotropy factor

(4) Use SIMSURF software (Herzfeld and Overbeck) to generate ice surface

(5) Sample model data sets for SB and MB data

(6) Analyze model data sets

The SIMFRACT method for simulation of scale-dependent fractal surfaces with natural roughness at each scale

(A) Data analysis part

(1) Calculate scale-dependent dimensions (a - Variogram method, b - Fourier method, c - Isarithm method)

(2) Determine homogeneity ranges of scale

(3) Determine anisotropies at each scale range

(B) Simulation part

(4)) Set up a simulation network, matching scale breaks

(5) Decide on scale ranges to interpolate versus ranges to simulate

(6) Select interpolation method (Shephard, 4-pt)

(7) Select simulation method (conditional, unconditional; using Fourier filter method for uncondl simulation of scale-dependent Fractional Brownian surfaces)

(8) Select a method to merge scales

Box dimension and isarithm method

The box dimension (a similarity dimension) of a bounded set $\mathcal{F} \subseteq \mathcal{R}^n$ is defined as

$$dim_B(\mathcal{F}) = lim_{\delta \to 0} \frac{\log N_\delta(\mathcal{F})}{-\log \delta} \tag{5}$$

(where $N_\delta(\mathcal{F})$ is the smallest number of sets of diameter at most δ needed to cover $\mathcal{F}$), if the lower and upper limes exist and coincide. It can be shown that the Hausdorff dimension is at most equal to the box dimension. The box dimension is usually estimated by regression of $\log N_\delta(\mathcal{F})$ versus $\log \delta$ (box-counting method).

The isarithm method is a similar method for surfaces in $\mathcal{R}^3$, it is fast but requires gridded data.

Functions with Hoelder conditions

PROPOSITION 6 (on functions satisfying Hoelder conditions): Let $f : [0,1] \to \mathcal{R}$ be a continuous function and $x_1, x_2 \epsilon [0,1]$.
(a) If there are $c_1, s \epsilon \mathcal{R}$ with $c_1 > 0$ and $1 \leq s \leq 2$ such that

$$|f(x_1) - f(x_2)| \leq c_1 |x_1 - x_2|^{2-s} \tag{8}$$

for all $x_1, x_2 \epsilon [0,1]$, then the Hausdorff measure $H^s(graph f)$ is finite and $dim_H(graph f) \leq dim_B(graph f) \leq s$.

(b) If there are c_2, δ_0, $s \epsilon \mathcal{R}$ with $c_2 > 0$ and $\delta_0 > 0$ and $1 \leq s \leq 2$ such that the following condition holds:
For each x_1 and $0 < \delta \leq \delta_0$ there is an x_2 with $|x_1 - x_2| < \delta$ and

$$|f(x_1) - f(x_2)| \geq c_2 \delta^{2-s} \tag{9}$$

then $s \leq dim_B(graph f) \leq dim_B(graph f)$.

PROPOSITION 8: Let $f : \mathcal{R} \rightarrow \mathcal{R}$ be a continuous function that satisfies the conditions in (a) and (b) of Proposition 6 for the same $s \epsilon \mathcal{R}$, and assume that the autocorrelation function $C(h)$ of f exists. Let $\gamma(h)$ denote the variogram of f, then:

$$\gamma(h) = 2[C(0) - C(h)] \approx c^2 h^{4-2s} \tag{15}$$

with $c_2 \leq \sqrt{2}c \leq c_1$ and $dim_B(graph f) = s$.

Variogram method for function graphs

PROPOSITION 9 (Variogram method for estimation of box dimension of graph of a real function): Let $f : \mathcal{R} \to \mathcal{R}$ be a continuous and self-affine function. Assume existence of the autocorrelation function C of f. Then there is a real number $c > 0$, such that

$$\gamma(h) = C(0) - C(h) \approx c\, h^{4-2s} \tag{22}$$

and $dim_B(graph f) = s$.

Under the condition of Proposition 8 above, the box dimension of f may be calculated according to

$$dim_B(graph\ f) = s \approx 2 - \frac{1}{2}\frac{\log(\gamma(h))}{\log(h)} + \frac{c}{\log(h)} \approx 2 - \frac{1}{2}\lim_{h\to 0}\frac{\log(\gamma(h))}{\log(h)} \tag{23}$$

which may be estimated using linear regression.

Variogram method in $\mathcal{R}^3$

REMARK 10 (Variogram method for estimation of box dimension for surfaces in $\mathcal{R}^3$): Let $(x,y)\epsilon\mathcal{D} \subseteq \mathcal{R}^2$, $f : \mathcal{D} \to \mathcal{R}$ an (elevation) function, and $\mathcal{S} = \{(x,y,z)|(x,y)\epsilon\mathcal{D}$ and $z = f(x,y)\}$. Let $d : \mathcal{R}^2 \to \mathcal{R}$ denote distance according to the L_2-norm. Assume $dim_B(\mathcal{S}) = dim_B(\mathcal{S} \cap \mathcal{T}) + 1$ for each intersection $\emptyset \neq \mathcal{S} \cap \mathcal{T}$ with a plane $\mathcal{T}$, and assume that the restriction $f|_{\mathcal{S}\cap\mathcal{T}}$ satisfies all the conditions of Propositions 8 and 9 above.
Then the following approximations hold:

$$\gamma(d(h)) = C(0) - C(d(h)) \approx cd(h)^{6-2s} \tag{24}$$

and

$$dim_B(\mathcal{S}) \approx 3 - \frac{1}{2} \lim_{d(h)\to 0} \frac{\log(\gamma(d(h)))}{\log(d(h))} \tag{25}$$

which may be estimated using linear regression.

Wiener-Kinchine Theorem

The Wiener-Kinchine theorem states that the power-spectral density is the Fourier transform of the autocorrelation function:

$$C(h) \rightleftharpoons |\Phi(p)|^2 = E_{SP}[f](p) \tag{32}$$

For two-dimensional functions, the Wiener-Kinchine theorem states that the power-spectral density is the Fourier transform of the covariance function.

Fourier method for function graphs

PROPOSITION 11 (Fourier method for calculation of box dimension for graph of a real function): Let $f : \mathcal{R} \to \mathcal{R}$ be a continuous and self-affine function, assume existence of the autocorrelation function C of f. Let $\Phi(p)$ denote the Fourier transform of f and E_{SP} the power-spectral density. If

$$E_{SP}[f](p) = |\Phi(p)|^2 \sim \frac{1}{p^\beta} \quad \text{for some } \beta \epsilon \mathcal{R}, \tag{33}$$

then

$$\beta \approx 5 - 2dim_B(graph\ f) \quad \text{and} \quad dim_B(graph\ f) \approx \frac{5-\beta}{2}. \tag{34}$$

Pine Island Glacier — L2A GLAS Data (2003)

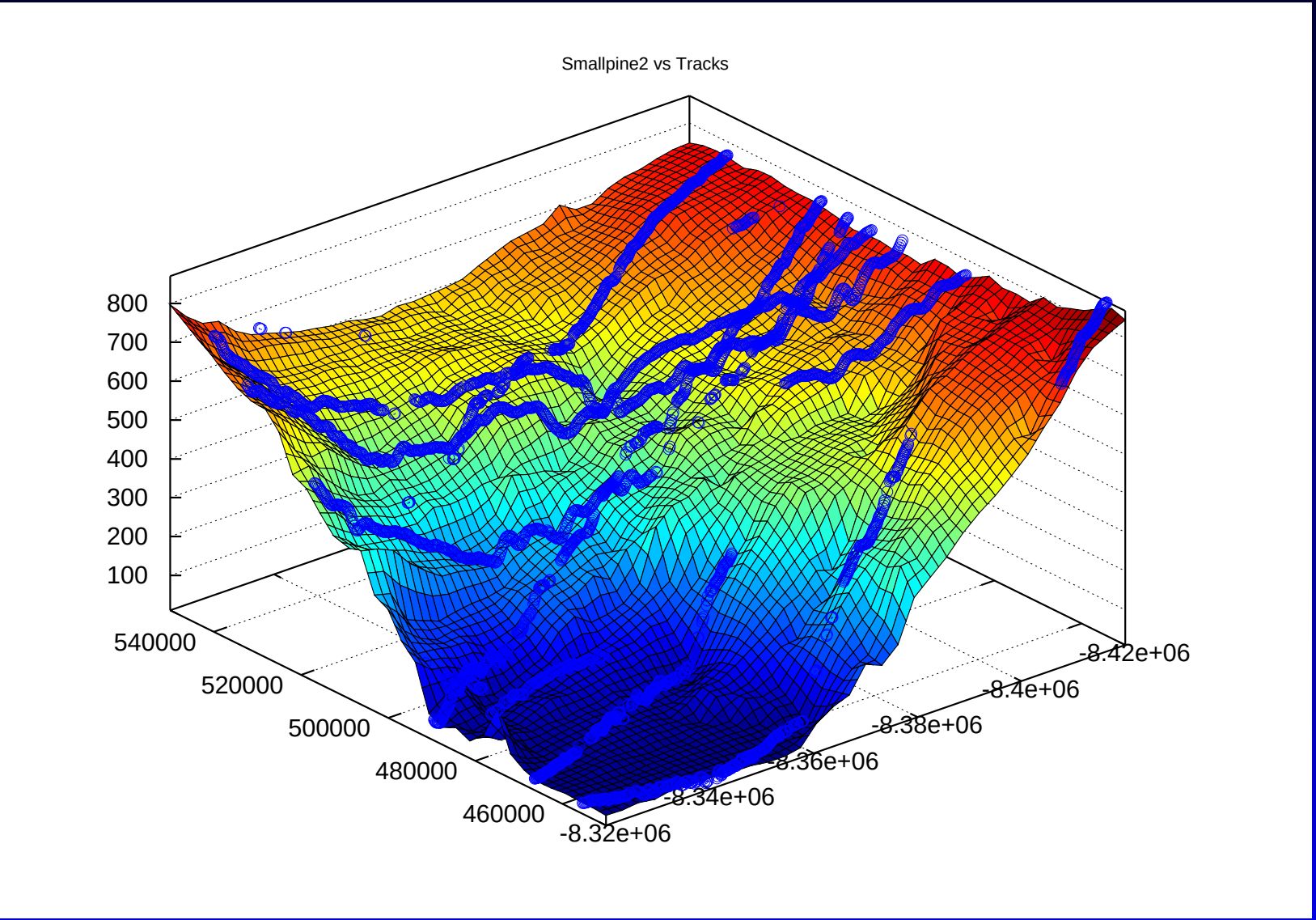

3D view upglacier, based on DEM from GLAS data, with GLAS data locations

Conditional Simulation: Pine Island Glacier

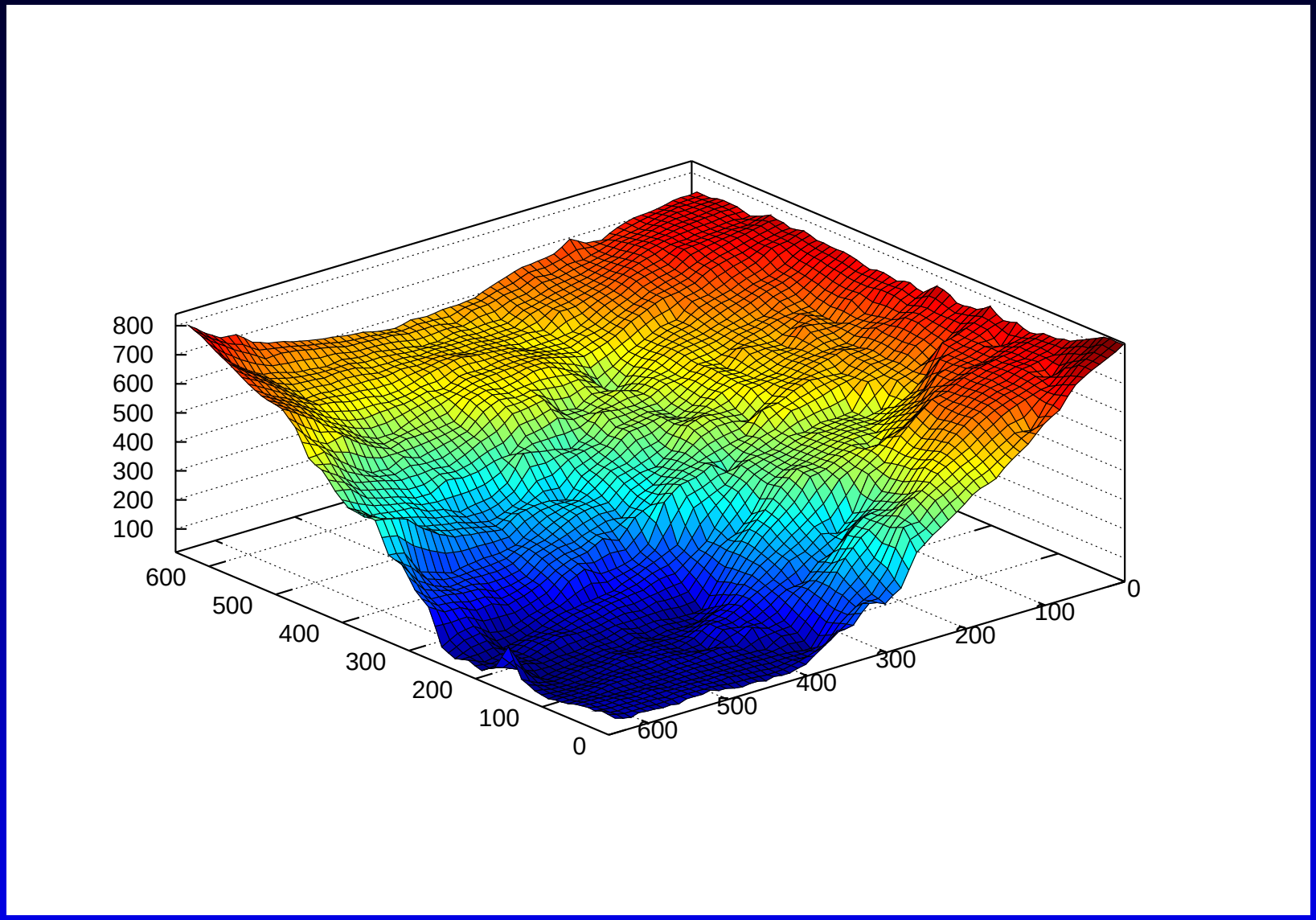

3D view upglacier, based on DEM from L2 (2003) GLAS data

Conditional Simulation: Pine Island Glacier – Enlarged Subarea

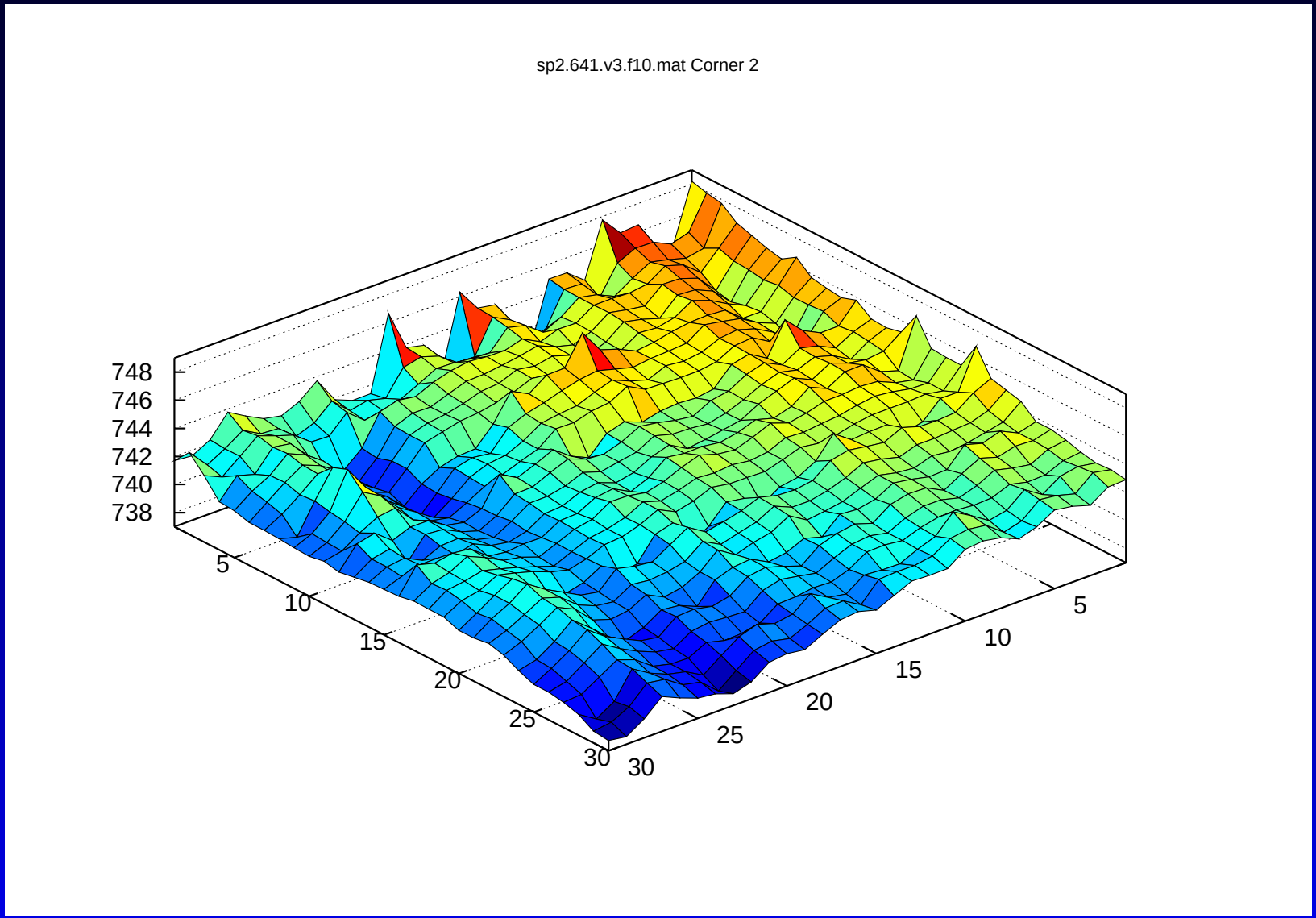

Gradient Map from Multi-Beam Data

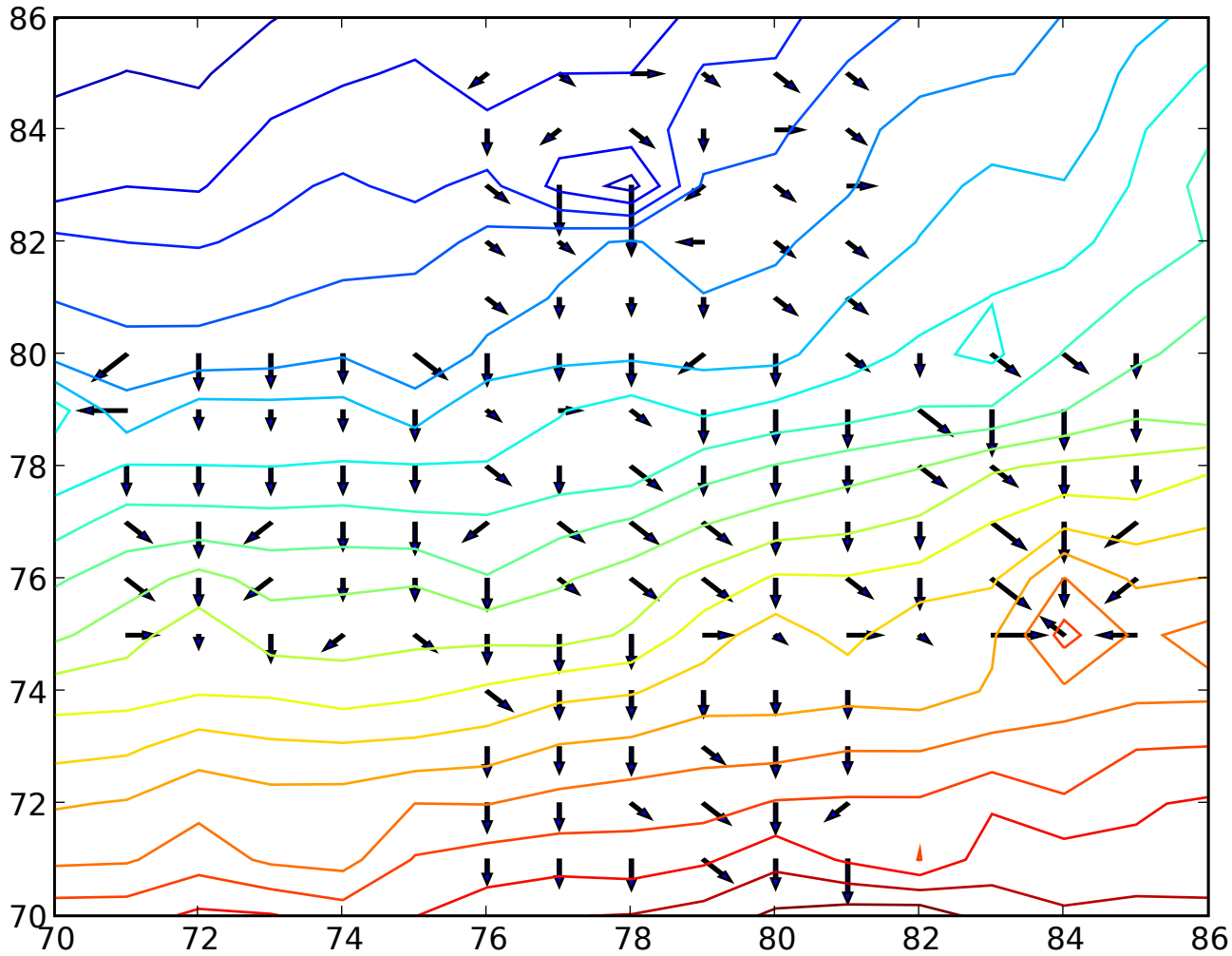

Histograms of Gradients

Objective: Investigate how well variability of surface slope is captured in SB and MB (8beam) observations

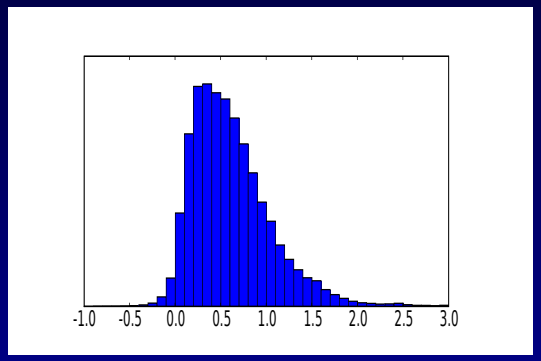

(A)

for MB data from Pinegl-Simul DEM (max. slope 4.3°)

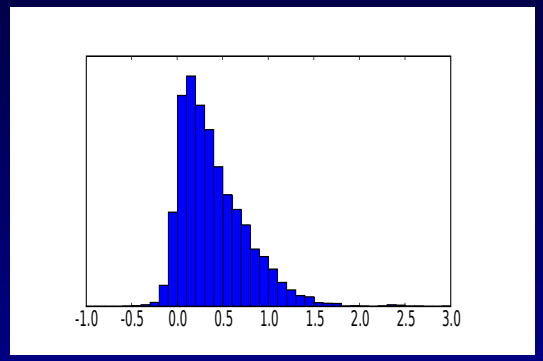

(B)

for SB data from Pinegl-Simul DEM (max. slope 2.9°)

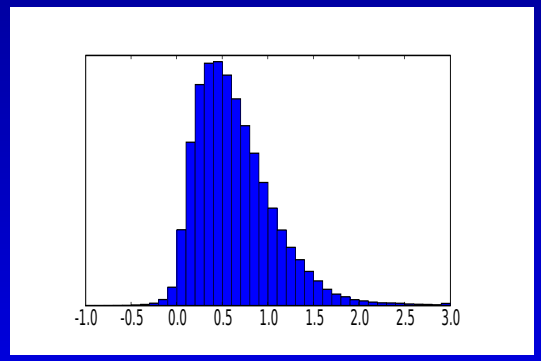

(C)

for entire Pinegl-Simul DEM. (max. slope 4.9°)

Sea Ice

Two components in a complex surface:

(1) rough surface

(2) segmented by leads

Analysis Approach:

(1) surface elevation and roughness
   - (a) from GLAS data analysis
   - (b) from snow-layer thickness and spatial roughness

(2) spatial distribution of leads
   - (a) lead distribution analysis (from Ron Kwok)
   - (b) lead distribution in SAR data

Sea Ice Simulation

Simulation Approach:

(1) surface elevation and roughness
  - create an unconditional simulation, using the SIMSURF software and fractal dimension, anisotropy direction and factor from GLAS data and snow-depth data

(2) spatial distribution of leads
  - combine simsurf with lead distribution in SAR data

Sea Ice Model Data Analysis

(1) select sample data sets for several beam configurations

(2) for each data set, calculate spatial statistical classification parameters

Lead Patterns 1: En echelon

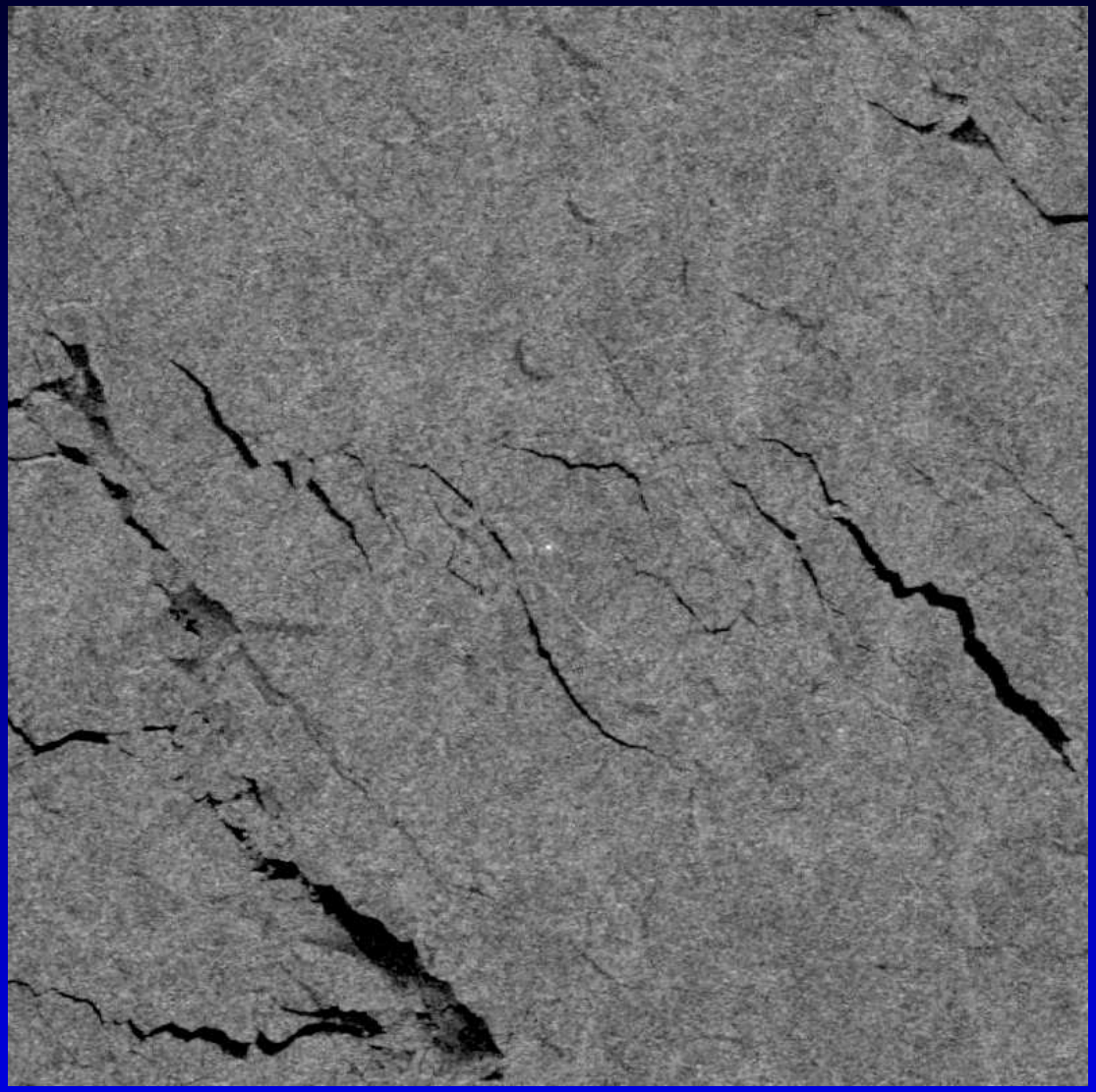

RADARSAT-1 SAR data (R110584186P3S010cal_center.eps),
SHEBA experiment, 50 m resolution, image $(40\ \mathrm{km})^2$,
processed by John Heinrichs

Lead Patterns 2:
2-D extensional and shear

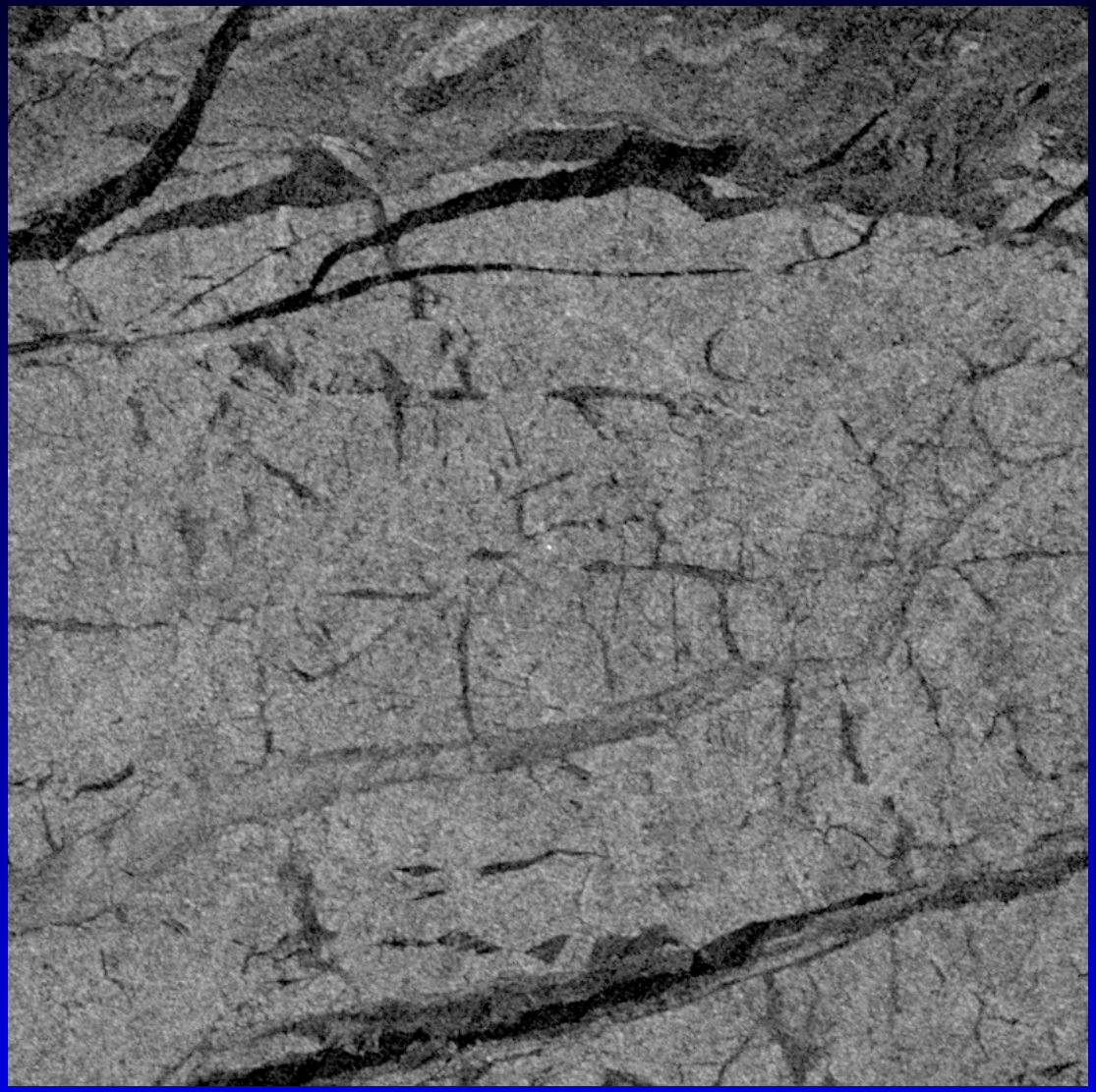

RADARSAT-1 SAR data (R111507261P3S016cal_center.eps),
SHEBA experiment, 50 m resolution, image $(40\ \mathrm{km})^2$,

processed by John Heinrichs

Lead Patterns - Binary

SAR data (R111507261P3S016cal_center.eps)

Lead Patterns - Subarea

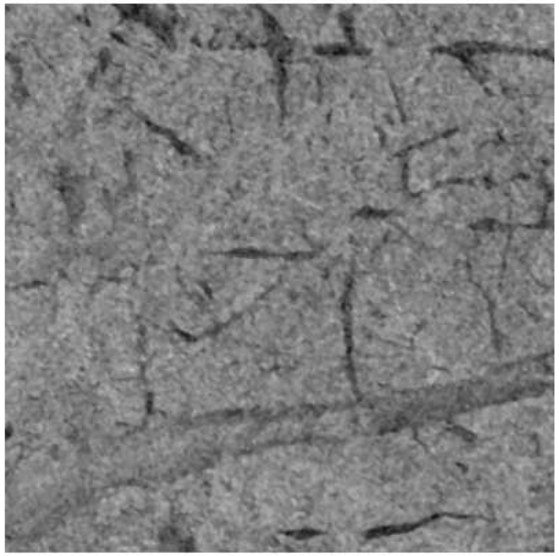

SAR data (R111507261P3S016cal_center.eps)

Simulated Sea Ice Surface with Leads

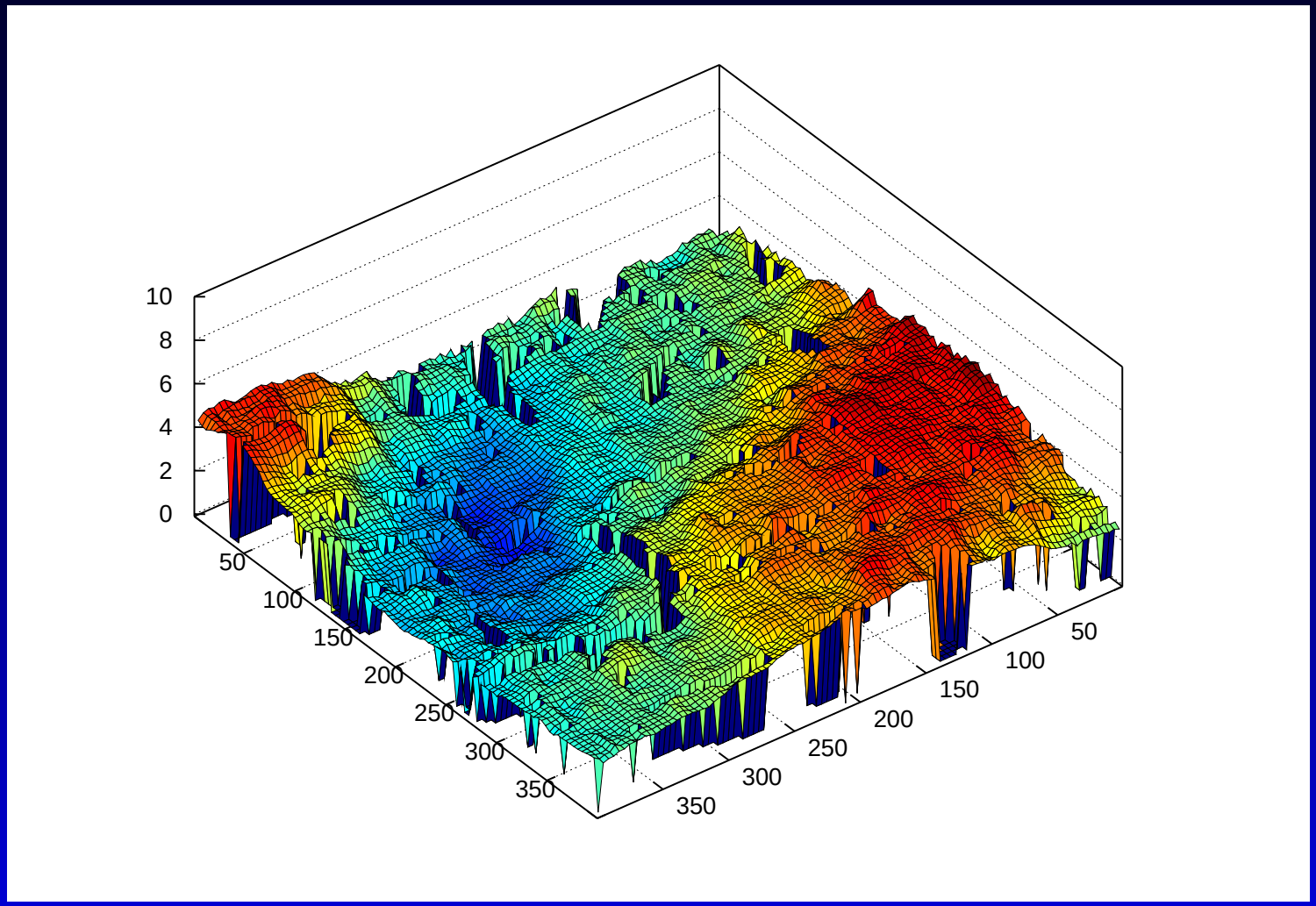

uncond simulation, fract dim 2.4, 2.1, 2.05, aniso 90° (1.9, 1.9, 0.5)
leads as in SAR data (R111507261P3S016cal_center.eps), 400x400 subarea
with 2-directional extensional kinematics

Questions?

Appendix

Algorithm V

Variogram method to estimate box dimension of a surface in $\mathbb{R}^3$

Let $(x, y) \in \mathcal{D} \subseteq \mathbb{R}^2, f : \mathcal{D} \to \mathbb{R}$ an (elevation) function, and

$\mathcal{S} = \{(x, y, z) | (x, y) \in \mathcal{D} \text{ and } z = f(x, y)\}$.

Let $d : \mathbb{R}^2 \to \mathbb{R}$ denote distance according to L_2-Norm.

(1.) Calculate experimental variograms in distance (k) and direction (α) classes (for global variogram, set tolerance angle $\beta = 180^o$):

$$\gamma(k) = \frac{1}{2n(k)} \sum_{i=1}^{n(k)} \sum_{j=i+1}^{n(k)} (f(X_i) - f(X_j))^2$$

for all pairs (X_i, X_j) with $d(X_i, X_j) \in [k - \frac{s}{2}, k + \frac{s}{2}[$,
and s the size of the distance class,
$X_i = (x_i, y_i)$, $X_j = (x_j, y_j) \in \mathcal{D}$,
and $X_i - X_j$ in direction class α,
$\arctan(X_i - X_j) \in [\alpha - \frac{\beta}{2}, \alpha + \frac{\beta}{2}[$.

(2.) Calculate coefficient u from regression of
$\log(\gamma(k))$ vs $\log(k)$

(3.) Estimate box dimension of $\mathcal{S}$ from

$$\dim_B(\mathcal{S}) = 3 - \frac{1}{2}u$$

Algorithm F

Fourier method to estimate box dimension of a surface in $\mathbb{R}^3$

The data describing the surface $\mathcal{S}$ are considered as contained in a rectangular grid with $N \times N$ nodes and a grid spacing of $\frac{1}{N-1} \times \frac{1}{N-1}$, after distance scaling. Let $f_{n,m} = f(x_n, y_m)$ denote the value of f at grid node (x_n, y_m), $n, m = 0, \ldots, N-1$.

(1.) Calculate two-dimensional Fourier coefficients $H_{s,t}$ $(s, t = 0, \ldots, N-1)$ using a discrete Fourier transformation

$$H_{s,t} = \sum_{n=0}^{N-1} \sum_{m=0}^{N-1} f_{n,m} e^{\frac{2\pi i}{N}(sn+tm)}$$

(2.) Calculate the average two-dimensional power spectral density E_{SP} according to

$$E_{SP}[f](j) = \frac{1}{N_j} \sum_{(s,t)\in\mathcal{I}_j} |H_{s,t}|^2$$

with $\mathcal{I}_j = \{(s,t) | j \leq r < j+1 \text{ and } r = \sqrt{s^2+t^2}\}$ and $N_j = |\mathcal{I}_j|$ the number of coefficients.

(3.) Calculate a regression coefficient w from regression of $\log E_j$ vs $\log j$ $(E_j = E_{SP}[f](j))$.

(4.) Estimate box dimension according to

$$\dim_B(\mathcal{S}) = \frac{7+w}{2}$$

Algorithm FL

Isarithm-type Fourier method to estimate box dimension of a surface in $\mathbb{R}^3$

Use notation as for algorithm F. $\mathcal{S}$ denotes the surface.

(1.) For each n, $n = 0, \ldots, N-1$, calculate one-dimensional Fourier coefficients according to

$$H_{j,n} = \sum_{m=0}^{N-1} f_{m,n} e^{\frac{2\pi i}{N} jm}$$

(2.) Calculate the one-dimensional power spectrum $E_{SP}[f_n]$ as

$$E_{SP}[f_n](j) = |H_{j,n}|^2$$

(3.) For each n, calculate a regression coefficient w_n from regression of $\log E_{SP}[f_n](j)$ vs $\log j$.

(4.) Estimate the box dimension of $\mathcal{S}$ according to

$$\dim_B(\mathcal{S}) = 1 + \frac{1}{N} \sum_{n=0}^{N-1} \frac{1}{2}(5 + w_n)$$

Algorithm FBS

Simulation of a fractional Brownian surface

with box dimension D

(1.) Generate a grid of $N \times N$ nodes with Gaussian random values $f_{n,m}$ for $n, m = 0, \ldots, N-1$, some $N \in I\!N$:

$$f(n,m) \sim N(0,1)$$

(2.) Calculate two-dimensional Fourier coefficients

$$H_{s,t} = \sum_{n=0}^{N-1} \sum_{m=0}^{N-1} f_{n,m}\, e^{\frac{2\pi i}{N}(sn+tm)}$$

for all $s, t = 0, \ldots, N-1$.

(3.) Filter Fourier coefficients with $\beta = 7 - 2D$:

$$H^*_{s,t} = \frac{1}{N_r} \frac{H_{s,t}}{r^{\frac{\beta}{2}}}$$

where $r = \mathrm{int}(\sqrt{s^2+t^2})$ the radial frequency
and N_r the number of coefficients $H_{s,t}$ with $r \leq \sqrt{s^2+t^2} < r+1$.

(4.) Apply two-dimensional inverse Fourier transformation:

$$f_{n,m} = \frac{1}{N^2} \sum_{t=0}^{N-1} \sum_{s=0}^{N-1} H^*_{s,t} e^{-\frac{2\pi i}{N}(sn+tm)}$$

Algorithm UCS

Unconditional simulation of scale-dependent surfaces merging fractional Brownian surfaces of different scales, dimensions, and anisotropic properties

(1.) Let $i = 1, B = 1, Z(n,m) = 0$ for $n, m = 0, \ldots, M-1$ and $N = \frac{sb1}{sb2}$, with $M \in I\!N$, $sb_1 = M$, and sb_2 the level of the first scale break.

(2.) Calculate B^2 fractional Brownian surfaces $f_{n,m}^{s \cdot B+t}$ for $n, m = 0, \ldots, N$ and dimension $D = \dim(i) = 3.5 - \frac{\beta(i)}{2}$ with $\beta \in [1,3]$, using algorithm FBS. Carry out backtransformation (step (4.) in FBS) using anisotropy factor according to Equation (47).

(3.) Merge new level grid with existing $M \times M$ grid:

$$Z^*(s \cdot sb_i + n \cdot sb_{i+1}, t \cdot sb_i + m \cdot sb_{i+1})$$

$$= Z(s \cdot sb_i + n \cdot sb_{i+1}, t \cdot sb_i + m \cdot sb_{i+1}) + v_i f_{n,m}^{s \cdot B+t}$$

$$n, m = 0, \ldots, N; \; s, t = 0, \ldots, B-1; \; sb_i \text{ scale break at level } i.$$

(4.) Calculate the trend imposed by the grid of higher level using 4-point method or Shepard method (including anisotropies, as in Equations (45) and (46), respectively).

(5.) Add up results of (3.) and (4.).

(6.) Set $i = i + 1, \; B = \frac{sb1}{sbi}, \; N = \frac{sbi}{sbi+1}$.

IF $i <$ number of scale **GOTO** (3.)
ELSE the surface is finished.